STOCHASTIC CONVEX OPTIMIZATION FOR REACTIVE POWER MANAGEMENT ON MICROGRIDS

Alexander Casilimas Peña

Thesis presented as a partial requirement
to qualify for the Master's Degree
in Electrical Engineering

Pereira, 27 November of 2019
UNIVERSIDAD TECNOLÓGICA DE PEREIRA
Master's Program in Electrical Engineering.

STOCHASTIC CONVEX OPTIMIZATION FOR REACTIVE POWER MANAGEMENT ON MICROGRIDS

Supervisor: Alejandro Garcés Ruiz.

Pereira, 27 November of 2019
Programa de Ingeniería Eléctrica.
Universidad Tecnológica de Pereira
La Julita. Pereira(Colombia)
TEL: (+57)(6)3137122
www.utp.edu.co
Versión web disponible en: *http://recursosbiblioteca.utp.edu.co/tesisd/index.html*

Dedicated to
my parents, my sister
and her unborn baby..."Gabo"

Acknowledgement

I would like to express my gratitude to my supervisor Alejandro Garcés Ruiz for the useful comments, remarks and engagement through the learning process of this master thesis. Also, I like to thank the members of both investigation groups CAFE and SIRIUS for their time, support, and help during the process of investigation and programming. I would like to thank my loved ones, who have supported me throughout entire process, both by keeping me harmonious and helping me putting pieces together. I will be grateful forever for your love and advice.

Abstract

This thesis document, presents a method for the optimal power factor calculation in power electronic converters for photovoltaic (PV) systems. Both three-phase and single-phase converters are considered through an unbalanced modeling of the grid. A Wirtinger's linearization is used for the power flow equations in order to obtain an affine set of constraint and make the problem convex. Stochastic behaviour of the solar radiation is considered by a sample average approximation which maintains the problem convex and computationally tractable. Numerical results performed in CVX/MATLAB on the CIGRE benchmark microgrid with real data of solar radiation, complement the analysis and demonstrate the applicability of the method. Beside this, the methodology of reactive power management mentioned before, allows to develop an algorithm, for *Hosting Capacity*, applying this on the CIGRE microgrid test benchmark, taking into account the behavior of the loads and sources both, balanced and unbalanced.

Table of Contents

Nomenclature

$\mathbb{E}(x)$ Expected value of the random variable x.

$\Omega(x)$ Set of feasible solutions.

ρ_k Auxiliar variable for the power factor calculation.

φ_k Power factor of the unit k

ξ_t Scenario of irradiance.

p_L Total power losses.

$p_{kG(max)}$ Maximum generated power in the converter connected to the node k.

p_{kG} Active power, generated at the converter connected at node k.

q_{kG} Reactive power generated at the converter connected at node k.

$s_{k(max)}$ Maximum capability of the converter connected to the node k.

v_k Voltage value in the node k.

v_{min}, v_{max} Minimum and maximum voltages allowed in the grid.

Y_{kk} Self-admittance of node k.

Y_{km} Mutual admittance between nodes k and m.

Chapter 1

Introduction

This thesis, presents a convex model for the defining the optimal value of power factor for PV systems. A series of convex approximations are proposed and evaluated. A three-phase modelling of the grid is proposed considering single and three-phase converters. Physical limitations of the converters are also considered and the grid equations are linearized by using Wirtinger's calculus. The stochastic behaviour of the solar radiation is considered by the sample average approximation in order to maintain the problem convex and computationally tractable. Real data for solar radiation are considered and applied to the CIGRE benchmark test system for low voltage applications [Papathanassiou et al., 2005]. Beside this, the application of this methodology allows to implement an algorithm to estimate and improve the hosting capacity, taking into account balanced and unbalanced loads.

Several methods were proposed before to solve this problem. In [Hamzeh et al., 2013], a decentralized self-adjusting reactive power controller was proposed, where the objective was to compensate the reactive power of local loads and share reactive power of non-local loads. That control included a drop constant that was adjusted according their reactive power. In [Bolognani and Zampieri, 2013], it was analyzed the system using a generalized dc power flow and quadratic programming obtaining an optimal reactive power flow that was used to control the reactive power supplied by each distributed generator. Reference [Zhu et al., 2016], proposed a wireless control strategy using optimized virtual impedance controllers and load measurements of reactive power sharing through the network, a genetic algorithm was used to define the virtual impedance parameters of each distributed generator which reduce the global reactive power sharing error. In [Arif et al., 2017], the authors presented the concept of stochastic game modelling from game theory to develop an algorithm to solve a multi-objective optimization, which included the reactive power reserve maximization and the improvement of voltage profile. Reference [Wang et al., 2017a], presented a control strat-

egy for islanded microgrids, using small signal models, state estimator, optimal regulator and an optimal control; all these allowed voltage regulation without communication systems. Authors in [Han et al., 2017] presented a review of multiple sharing strategies of active and reactive power in hierarchical controlled microgrids. [Morais et al., 2013] mentioned multiple reactive power control strategies considering the smart grids paradigm. The management of distributed energy resources and the distributed network aggregator, namely Virtual Power Player, was proposed and implemented in a simulation tool. In [Águila Téllez et al., 2018] it was proposed a bibliographical revision of mathematical methods used for optimal selection and location of reactive power compensating elements applied on distribution systems most of them based on metaheuristics. There are a few articles that study the stochastic nature of renewable resources and load on microgrids, some like [Kekatos et al., 2015], did a mathematical analysis of the components and stochastic behavior of the system to obtain an optimal power flow and reduce losses. That model was however, non-convex and hence, there was not guarantee of optimally or convergence.

The main differences between the aforementioned approaches and the one presented here are the following: i) the proposed model is convexified by using a Wirtinger's linearization on the power flow equations [D.A.Ramirez et al., 2019]. This linearization allows to guarantee global optimum in the approximated model with high accuracy and fast convergence of the interior point algorithms. ii) The proposed model consider directly the stochastic behaviour of the solar generation by using a sample average approximation. This approximation takes into account the stochastic nature of the sun radiation and the loads, without jeopardize the convergence and uniqueness properties of the convex model. iii) The implementation of the proposed methodology can be executed directly in commercial converters, since it does not require communications or real time operation. The main idea of this, is to schedule the power factor of the converter for each type of day and each hour without a master controller.

1.1 Problem description

Modern distribution systems are characterized by a high penetration of renewable energy such as wind and photovoltaics, which are integrated through power electronic converters [Rabiul Islam et al., 2019]. Although these converters have some power factor compensation capability, they are usually operated at unit power factor; this operation mode can reduce the efficiency of the entire system [Lu et al., 2015]. One of the most promising ways to solve this problem is by including communications and a power factor management in real time. However, this approach is still expensive in practical applications. Therefore, an optimization model for the power factor is required in order to define a fixed set point taking into

account the stochastic behaviour of the solar generation. The electrical sector is one of the main responsible or global warming and air pollution. Hydroelectrics create a high social and environmental impact, and the abusive use of coil, gas, and diesel, increased drastically the CO2 emissions and the greenhouse effect. With this in mind, scientist start developing renewable energy technologies such as solar and wind farms. The integration of these elements and others like energy storage devices, requires the concept of microgrid, defined as an interconnection of distributed energy resources (DER's) creating small distributed systems that can operate on interconnected or islanded mode. These renewable systems, have power electronics elements mainly converters with the capability to control the reactive power injected to the grid. We should establish the optimal power reactive point, however, there is a limit for the current that may inject to the grid and hence the available reactive power is closely related to the active power capability.
Controlling the operation point is important because on situations where the voltage drops or rises, those devices must generate or consume reactive power. However, microgrids and in general renewable energy resources have an inherent stochastic characteristic. It means that on microgrids the load is variant and the energy produced by solar farms is difficult to predict, that is because the solar radiation is variable throw the time; the same happens with the unpredictability nature of wind speed on wind systems. With this in mind and interrogant born. ***How to control the reactive power on microgrids with high inclusion of renewable energy, in order to optimize the operation and taking into account the stochast nature of the solar irrandiance?***

Solving this problem becomes difficult unless we use optimization methods than include the stochastic nature of renewable resources and loads. In this document, it is going to be used stochastic convex optimization. The purpose of using convex optimization is to take advantages that other mathematical process like metaheuristics do not have. The main advantage is that the solution point is unique and global. In addition, convex models have a convergence gurantee for conventional methods such as the interior point method. This means, that the model is solver-agnostic (i.e it does not depend on the solver used to be solved). However, not all problems are convex and our particular problem is not an exception, because the power flow equations are highly non-liner and non-convex, and the constant power model of solar systems are non-linear. In those cases, it is needed a relaxation of the problem. It means that the model is converted into a convex model and after that, we can use technological tools like Matlab and CVX to solve the problem and find the optimal point.

1.2 Motivation

The development of grids with high penetration of distributed generation has become important for the future of the electrical systems due to the increase of pollution and the continuous emission of greenhouse gasses. Microgrids have advantages over the traditional power systems such as, reduced feeder losses and improved power system quality and reliability [Han et al., 2017]. The active elements on microgrids, such us solar panels, wind generators, storage devices, and loads, are normally connected through power-electronic converters. These devices have the capability to generate or consume reactive power as long as the maximum current capability is not violated. Therefore, an optimization model is required for the optimal power factor calculation.

On traditional power grids, a few number of elements where in charge of generating power. Coordination in those green was relatively easy, but on microgrids with high inclusion of renewable energy, we have multiple distributed resources with a variable generation during the day, each one connected to the grid using power electronics devices. These devices, when not properly controlled, increase the feeder voltage because of their reverse power flow. Here the reactive power has a key role on maintaining the proper voltage grid profiles. Other power quality problems normally are to be mitigated by providing harmonic, reactive power and unbalanced compensation. Reactive power problems cause disturbance to other consumers an interference in nearby communication networks, but different compensation devices are presented as a solution to reactive power compensation [Gayatri et al., 2018].

The use of capacitor banks are useful to mitigate power quality problems. Also the use of LC-filters helps reducing the number of capacitor banks while improving the power factor. However, those devices do not help with resonance, bulkiness or fixed compensation. Others like flexible alternating current transmission systems (FACTS) have been proposed on microgrids as a complete solution, but those are expensive and becomes difficult to implement in microgrids, so the target now is to use the capability that existing power electronic devices, have to control the active and reactive power.

The use of optimization techniques to control the operation of the inverters is an excellent solution to replace the use of capacitor banks that have a limited capacitance level, meanwhile the control over the converters helps on network stability by consuming or generating reactive power, which in turns helps to keep the voltage in normal values [Garces et al., 2012].

In our study, it is required a variability model of the solar radiation and the magnitude of the load. It means that generation and demand is changing through the time.

1.3 Objectives

1.3.1 General

To develop a stochastic convex optimization methodology that manage the reactive power in electronic devices (AC/AC, DC/AC converter), that integrate renewable energy taking into account the variability of the load and the renewable resources (solar radiation, wind frequency).

1.3.2 Specific

- Modelling both sources and loads through a suitable models.
- To purpose a convex model for optimal management of microgrids.
- To solve the optimization problem through an algorithm implemented in MatLab.
- To analyze results on a test system.
- To include an algorithm for hosting capacity using reactive power management.

1.4 Research framework

1.4.1 Microgrids

The different connections between photovoltaic, wind, storage systems, fuel cells and other cross-cutting technologies are normally defined as distributed energy resources (DER) and the interconnection of multiple DER is called microgrid [Bullich-Massagué et al., 2018]. The development of microgrids is closely related to the development of the smartgrids [Razeghi et al., 2018]. A microgrid basically takes a community that is interconnected with the different smartgrids technologies and uses different types of energy generation and storage, to produce energy to supply themselves and also deliver the residual energy to a main grid.

At distribution level, the grids work as passive systems, but the integration of distributed resources make the system dynamic with own control and with a bidirectional power flow. It means that the micro grid can work as a load for the main system, but it also can work as a generator supplying energy. Normally, microgrids are low (inferior to 1 kV) or medium voltage (1-69 kV) and they can operate in two modes [Bullich-Massagué et al., 2018]:

Connected mode: In this mode in which the microgrid is connected to a main grid, where it can supply energy to the system and also consume energy from it.

Isolated or islanded mode: on this mode the grid is completely autonomous generating their own energy and is not connected to a main grid.

With the environmental philosophy in recent years, photovoltaic and wind became an important part of the system. Photovoltaic energy that normally uses poly-crystalline solar cells on their solar farms had the problem of poor prediction of solar radiation over the time.

Those uncertainties, as well as the load variation, represent a challenge for the system operators. It is required a control to guarantee power quality and security of supply. These stochastic approach are used for optimal operation, the strategies include scenario trees for stochastic variables (wind frequency, solar radiation), that are integrated to optimization problems [Grover-Silva et al., 2018].

1.4.2 Convex optimization

Convex optimization is a mathematical process with high differences respect to metaheuristics optimization and benefits like global solutions and multiple programs to solve effectively the problems. Convex optimization includes linear programming problems, semi-definite and second order cone programs almost as easily as linear programs. Since 1990, multiple applications have been discovered, like automatics, finances, signal processing and more. The advantages of recognizing or formulating a problem as a convex optimization model are: simplicity, since the problem can be solved very reliably and efficiently and the methodologies can be easily embedded in a computer or analysis tool. Basically solve convex functions over convex regions [Boyd and Vandenberghe, 2004]. In our problem of reactive power management, the system generates non-convex function that could not be possible to solve using convex optimization, in that case it is needed a methodology of relaxation that change the problem from non-convex to convex. In Chapter 2, the application of convex optimization for the solution of load flow optimization problems will be thoroughly studied

1.4.3 Stochastic models for wind and sun radiation

Stochastic process are related to probability theory, involved in many phenomena's like physics, engineering, ecology, biology, medicine, psychology, finance and other disciplines. A stochastic process is defined as a collection of random variables that are continuously changing over the time. Each random variable, has their own probability distribution function that could be or not related between them.

It is important than a stochastic process to be generated should resemble its estimated statistical and probabilistic properties. For a random variable its probability distribution is a complete description. For a stochastic process, two properties have been used for that purpose: the probability distribution and the power spectral density. The first one is the property at one time instant, and it is the first order property of the process. The second one, in the other hand is a statistical property involving two different time instants, both the probability distribution and the power spectral density are invariant with time [Cai, 2018].

1.4.4 Hosting capacity

On distributed systems, the hosting capacity is the ability that Distributed energy resources (DER) had to identify the penetration level of generation resources that can be accepted without endangering the power quality and the state of the grid [Etherden and J.Bollen, 2011]. Often the main problems associated with a lack of hosting capacity are related to voltage problems like overvoltage, undervoltage and voltage deviation, thermal problems like charging overloads and discharging overloads and finally protection problems like sympathetic tripping, coordination and reverse power flow [Rylander et al., 2016].

1.4.5 State of art

There are little information about power reactive management on microgrids, most of the information is focused on transmission systems. In this section is going to be presented some of the studies developed on microgrids for reactive control management:

[Hamzeh et al., 2013], it is presented a decentralized self-adjusting reactive power controller, the main objective was to develop a control for each distributed generation unit, to compensate the reactive power of its local loads and share reactive power of non local loads. The proposed control includes an improved drop controller whose parameters are adjusted according of the reactive power of the loads, a virtual impedance loop is added to the voltage controller to enhance the steady state and transient responses of the proposed reactive power management scheme. [Morais et al., 2013] mentioned multiple reactive power control strategies considering the smart grids paradigm. The management of distributed energy resources and the distributed network aggregator, namely Virtual Power Player(VPP), was proposed and implemented in a simulation tool designed for the paper's author.

In [Kekatos et al., 2015], a reactive power compensation was considered as an auxiliary service, taking into account the increasing time-variability of distributed generation and demand. A stochastic reactive power compensation scheme is developed, given uncertain active power injections. Reactive power injections are updated using the Lagrange multipliers

of a second-order cone programming, being capable to track variations in solar generation and household demand.

[Guo et al., 2019] proposed a distributed coordinated active and reactive power control scheme for wind farms based on the model predictive control (MPC) along with the consensus-based distributed information synchronization and estimation, which can optimally dispatch the active power of wind turbines (WT) and regulate the voltages within the wind farm. The reactive power outputs of WTs are controlled to mitigate the voltage deviations and simultaneously optimize reactive power sharing.

In [Águila Téllez et al., 2018], it was proposed a bibliographical revision of mathematical methods used for optimal selection and location of reactive power compensating elements applied on distribution systems most of them based on metaheuristics. [Torquato et al., 2018] Proposed the application of a simplified Monte-Carlo method applied on 50.000 low voltage systems where they perform a risk-based analysis, here they found that the highest impact on microgrid with high inclusion PV is the overvoltage. In [Wang et al., 2017b], it was presented an study for hosting capacity on grids with inclusion of wind turbines on the mathematical model raised is included economical and installation points restrictions which was solved using particle swarm optimization. [Rylander et al., 2016] proposed a streamlined methodology that captures characteristics from the electric providers and consumers and run multiple load-flows and short-circuit analyses to provide the ability to the feeder to accommodate multiple PV on the grid. [Wang et al., 2016] used the IEEE-33 bus distribution system, realize an study taking into account the inclusion of on-line tap changers (OLTC) and static var compensators (SVC's), with this is discussed how to find the most critical technical constraints that may limit the maximum hosting capacity adjusting those parameters to increase the effectiveness of the mathematical formulation.

1.5 Scope and investigation products

In this project a stochastic convex optimization mathematical model is proposed on microgrids with high inclusion of distributed generators (DG). The load flow methodology used will be linearized load flow for distributed networks; this methodology is helpful because it deliver direct responses in magnitude and phase. The DG composed by multiple solar panels, is considered the generation variability of solar radiation and load.

With this in mind and taking into account the benefits of power factor control, we will focus our project on the magnitude of capacity of solar generators that a grid can hold on without producing effects on it like over/under voltage, conductor heating and overload on transformers. This optimal sizing of distributed generators on a microgrid is named *Hosting*

Capacity. Next, will be shown information about studies that work on the improvement of the hosting capacity on DER's.

The following are main products of the thesis:

- Paper conference presented in international congress CIINDET (*Congreso internacional de innovación y desarrollo tecnológico*) Cuernavaca - Morelos October of 2019 [Casilimas et al., 2019].
- Test system based on the CIGRE test benchmark.
- Matlab optimization model implemented on CVX.

1.6 Structure of the Thesis

This thesis project is organized as follows. Chapter 2 explains and defines stochastic programming and define the multiple constraints used on our *Optimal Power Flow model*. Chapter 3 is defines the mathematical model of the grid, in which the main objective is loss reduction where are defined the system constraints, also is presented Wirtinger's linearization as a methodology to linearize non-convex constraints and finally stochastic model parameters are determined which allow us use convex optimization and CVX/MatLab to perform reactive power management. Chapter 4 are presented two types of results, the first ones are for reactive power control which is compared with a deterministic experiment and the second one present results for hosting capacity. Chapter 5, display the main conclusions and final observations from the simulations also present the future works coming from this investigation thesis.

Chapter 2

Non-convex stochastic model

2.1 Stochastic modelling

Stochastic programming deals with optimization models and decision making involving uncertainty [Lin et al., 2012]. These optimization problems present greater challenges compared to deterministic models. Stochastic programming includes different methodologies and approaches that represent the uncertainty (See [Bhattacharya et al., 2018] and [Hanhuawei et al., 2017] for more details about stochastic modelling). In general, the objective function is replaced by a measure over the feasible set consider the stochastic nature of the problem. The most common approach, is to use the expected value of an objective function, namely:

$$\min \ \mathbb{E}(f(x)) : x \in \Omega(x) \tag{2.1}$$

However, finding the expect value could be difficult taking into account the possible nonlinear characteristics of the objective function f and/or the set of feasible solutions Ω. In order to solve this problem, is to perform an analysis of scenarios. Here, the main idea is to make a study in a set of possible scenarios or realizations (ξ_i) with their corresponding probabilities and with them, give a solutions to the problem [Kall and Wallace, 1994].

The decision making in a stochastic model, can be performed in one or several stages. In the first case, named single stage stochastic optimization, the decision is implemented with no subsequent recourse. This strategy is called here and now. In the second case, part of the decision is taken by stages after obtained a given realization. This strategy is called wait and see. The optimization model presented in this thesis is a single stage stochastic optimization where the decision of the power factor is fixed in by the model.

2.2 Solar system model

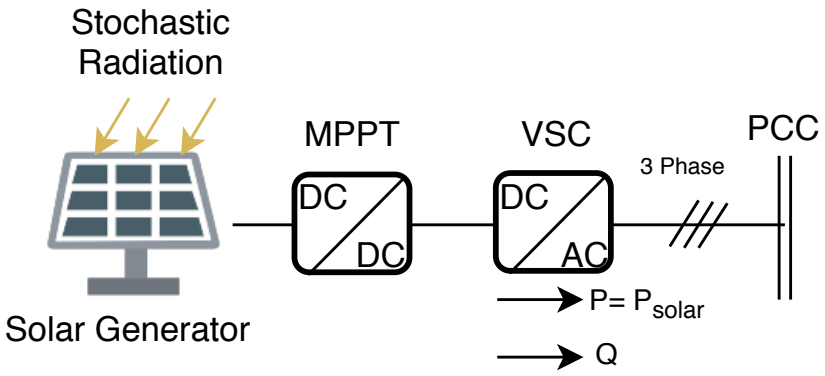

Figure 2.1: Solar Power Plant Configuration

Figure 2.1 presents the basic configuration of a solar generation system, which will be our primary source of study. This system consists on a group of solar panels whose capacity is variable depending on the size of the installation, the number of panels and their technology. The second element of this installation is a DC/DC voltage regulator of type maximum power point type tracker (MPPT), these systems are used in high voltage installations, in addition to this, they have a better efficiency than the pulse width modulation type regulators (PWM), this element connects and stabilizes the voltage between the solar panels and the DC/AC converter.
The next element of the solar generator is the DC/AC source converter of the voltage source converter type (VSC). This converter which gives us the active power directly from the panels and allows to consume or inject reactive power to the grid through the control of the switch of its electronic components, will be the most important element in our study, since these allows control through user access panels or acquisition cards the behavior of the power factor during the day. That power factor will be the parameter which our study is dedicated to obtaining its optimum values for dynamic conditions of the network. Finally this solar system which now is three-phase, is connected to the system by the point of common coupling (PCC).

2.3 Optimal Power Flow (OPF)

Let us consider a grid-connected three-phase microgrid as depicted in Figure 2.2. This consist in a slack node which maintains a constant three-phase voltage, distribution lines and loads.

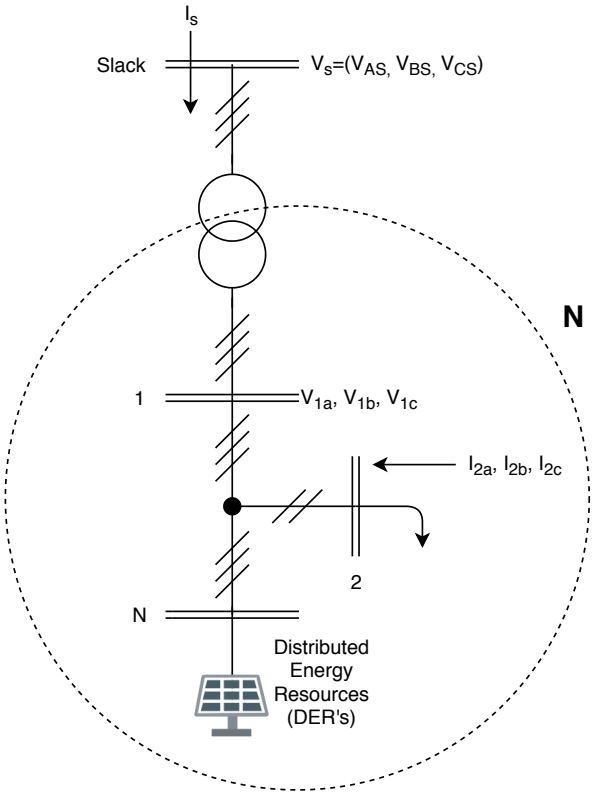

Figure 2.2: Representation of a three-phase Grid

Distributed energy resources (DERs) are connected to different nodes. In this case, these we consider only photovoltaic. Our problem is to obtain the optimal power factor for each photovoltaic unit in each our in order to minimize the expected value of the losses.

This problem is closely related to the optimal power flow (OPF) in power systems (see [Conejo and Baringo, 2017]). In the following, the objective function as well as the set of constraints are presented in order to built the optimization model.

2.3.1 Objective Function

The proposed model seeks to find the optimal power factor for each solar conversion system, in order to minimize power loss. However, losses depends both the power factor and the scenario of solar irrandance and loads. Therefore, the objective function is to minimiza the expected value of the losses as given in (2.2)

$$\min \ \mathbb{E}(p_L, \xi_t) \tag{2.2}$$

The losses are represented by a quadratic form as function of voltages and the parameters of the grid, as well as the scenario of solar radiation as will be explained later.

2.3.2 Power balance

For the sake of simplicity, the model of the grid is presented in a complex representation. The power that flows across the network branches is therefore represented by the following non-linear / non-affine model:

$$\left(\frac{s_k}{v_k}\right)^* = \sum_m y_{km} v_m \tag{2.3}$$

where $*$ represents the complex conjugate operator, v_k, v_m are nodal voltages and y_{km} is the component km of the nodal admittance matrix. The nodal power in each node is given by $s_k = s_{kG} - s_{kD}$ where $s_{kG} = p_{kG} + jq_{kG})$ is the generated power and loads are given by $s_{kD} = p_{kD} + jq_{kD}$. Therefore, the model of each node is given by (2.4).

$$(p_{kG} - p_{kD}) - j(q_{kG} - q_{kD}) = \sum_m v_k^* y_{km} v_m \tag{2.4}$$

The total active power loss are given by the sum of the nodal powers, namely

$$p_L = \sum_k \sum_m \text{real}(v_k^* y_{km} v_m) \tag{2.5}$$

This is a quadratic and convex form since we assume the graph is connected.

2.3.3 Voltage magnitude limits

This constraint limits the maximum (v_{max}^k) and minimum (v_{min}^k) values of voltages on all the nodes of the system.

$$v_{min}^k \leq \|v_k\| \leq v_{max}^k \tag{2.6}$$

These limits are given by the grid-codes. In Colombia, it is used a range of $\pm 10\%$. that implies that $v_{min}^k = 0.9$pu and $v_{max}^k = 1.1$pu

2.3.4 Slack nodes

There are three slack nodes, one of each phase of the grid as given in (2.7)

$$V_S = \begin{pmatrix} V_{A(slack)} \\ V_{B(slack)} \\ V_{C(slack)} \end{pmatrix} \tag{2.7}$$

This vector is a parameter of the model, therefore, we can represent the following constraint in per unit:

$$v_{\text{slack}} = 1e^{j\phi} \tag{2.8}$$

where $\phi \in \{0, -2\pi/3, 2\pi/3\}$ according to the phase of the grid.

2.3.5 Active and reactive power generation

This constraint relates the apparent power in active and reactive power of all the generation nodes with the maximum value of apparent power than the solar generator converters can inject to the grid as given in Equation (2.9).

$$\sqrt{p_{kG}^2 + q_{kG}^2} \leq s_{k(max)} \tag{2.9}$$

The capacity of the converter is given mainly, by the current capacity of the Insulated Gate Bipolar Transistors (IGBT). This parameter can be obtained from the datasheet of the converter.

2.3.6 Active power limiter

Equation (2.10), as a secondary constraint of the restriction above, limits the magnitude of active power injected to the grid depending on the active power produced by the solar panels at a statistical case and a specific radiation level.

$$p_{kG} \leq p_{kG(max)}(\xi_t) \tag{2.10}$$

The parameter ξ_t represents the scenario of solar radiation. Therefore, this constraint is probabilistic, unless if a precise forecasting is available.

2.3.7 Power factor

The power factor of the solar units is given by

$$\varphi_k = \frac{p_{kG}}{\|s_{kG}\|} \tag{2.11}$$

For the sake of simplicity, an artificial variable ρ_k is created and defined as follows:

$$\rho = \sqrt{(1/\varphi_k^2) - 1} \tag{2.12}$$

Therefore, reactive can be represented as function of the active power, namely:

$$q_{kG} = \rho_k p_{kG} \tag{2.13}$$

This variable will be used by optimization model and the power factor given by (2.12) will be calculated offline, after the model achieves an optimal solution.

2.4 Formulation of the non-convex model

For the sake of completeness, the model is presented below. This consists on minimizing the expected value of total losses p_L subject to technical constrains as presented below.

Model 1 *Complete model for the optimal set point of the reactive power in a three-phase grid is organized as follows:*

$$\min \mathbb{E}(p_L, \xi_t) \tag{2.14}$$

$$(p_{kG} - p_{kD}) - j(q_{kG} - q_{kD}) = \sum_m v_k^* y_{km} v_m \tag{2.15}$$

$$v_{slack} = 1e^{j\phi} \tag{2.16}$$

$$v_{min} \leq \|v_k\| \leq v_{max} \tag{2.17}$$

$$\sqrt{p_{kG}^2 + q_{kG}^2} \leq s_{k(max)} \tag{2.18}$$

$$p_{kG} = p_{kG(max)}(\xi_t) \tag{2.19}$$

$$q_{kG} = \rho_k p_{kG} \tag{2.20}$$

where (2.14), is a convex function that represents the expected losses of the network, (2.15) are non-linear and non-convex equations that represent the active and reactive power flow constraints respectively, (2.17) is the maximum and minimum voltage of the grid, (2.18) is the capability of the converter and (2.19) is the maximum power that can be generated in each node. Notice that (2.18) depends on the converter whereas (2.19) depends on the primary resource (i.e the scenario of the irradiance ξ_t). Therefore, $p_{kG(max)}$ is a random variable. It is important to note that (2.15) is maintained in complex form for the sake of a simple representation. However, this equation requires to be separated into real and imaginary parts.

This problem is difficult to solve due to the non-linear non-convex nature of the power flow equations but also due to the stochastic nature of the model. In the next chapter, the model is simplified for a deterministic case in order to obtain a convex model (see [Boyd and Vandenberghe, 2004] for a formal definition of convexity).

Chapter 3

Stochastic convex optimization model

3.1 Convex optimization

Before presenting the main result of the thesis, let us review some basic concepts from convex optimization:

Convex function: A real-valued function $f : \mathbb{R}^n \to \mathbb{R}$ is convex if its domain is convex and for any two points $x, y \in \mathbb{R}^n$ we have that

$$f(\lambda x + (1-\lambda)y) \leq \lambda f(x) + (1-\lambda)f(y) \tag{3.1}$$

for all $\lambda \in \mathbb{R}$ such that $0 \leq \lambda \leq 1$.Intuitively, all points in a line segment of a convex set belong to the set as depicted in Figure 3.1a.

Convex set: We say that a set $\Omega \subset \mathbb{R}^n$ is convex if for any $x, y \in \Omega$ we have that

$$(1-\lambda)x + \lambda y \in \Omega \tag{3.2}$$

for all $\lambda \in \mathbb{R},\ 0 \leq \lambda \leq 1$. Graphically, a convex function is a real valued function in which it is possible to draw a line above the function for a given interval as depicted in Figure 3.1b.

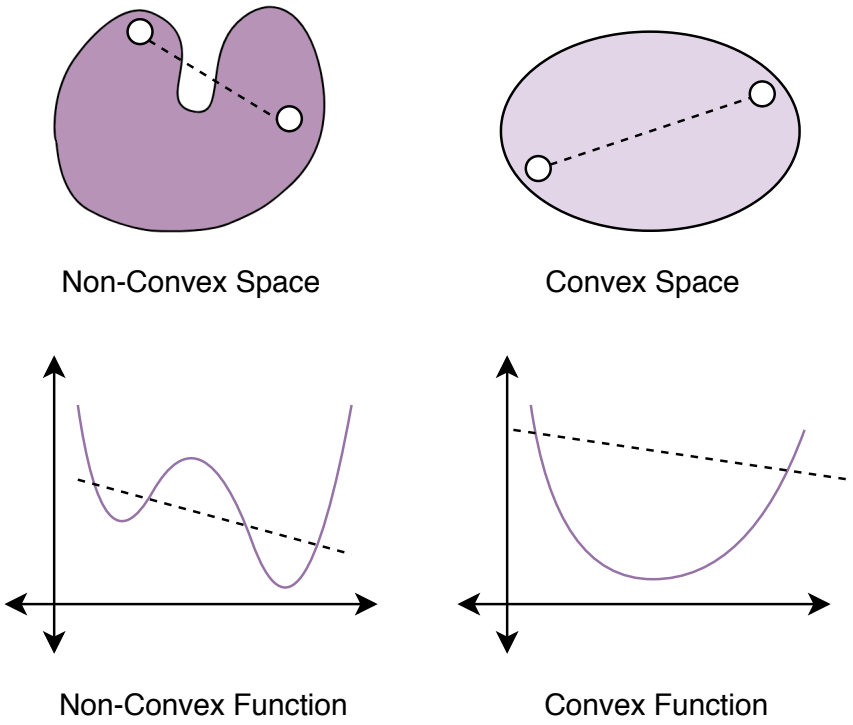

Figure 3.1: Example of a convex function and a convex set

As mentioned before, convex optimization deals with deterministic optimization problems as follows:

$$\min \ f(x) : x \in \Omega(x) \tag{3.3}$$

where $f : \mathbb{R}^n \to \mathbb{R}$ is a convex function and $\Omega(x)$ is a convex set that can be represented as a set of constrains as given below:

$$\Omega(x) = \left\{ \begin{array}{l} h_i(x) = 0 \\ g_i(x) \leq 0 \end{array} \right\} \tag{3.4}$$

where equality constraints h_i are affine or linear and innequality contraints g_i are convex functions.

Convex optimization models have many theoretical and practical features which are suitable for optimization in power distribution grids. One of this important features is the guarantee of the global optimum, convergence of the interior point methods and, in some cases, uniqueness of the solution.

As a single unit, Model 1 presented before is non-convex, however, some of the constraints are convex. Therfore, the model is suitable to be convexified. The main challenge are the power flow equations. These requiere a linearization as presented in the next section.

3.2 Power flow linearization

The problem of non-convexity and non-linearity mentioned before has to be relaxed in order to obtain a tractable model. There are different linearizations proposed in the literature standing out the one presented by Bolognani [Bolognani and Zampieri, 2016], Marti [Martí et al., 2013] and Garcés [Garces, 2016]. Although each of these linearizations comes from a different theoretical background. The first approximation is an application of the Banach fixed point theorem, the second is a curve-fitting and the third is a Taylor expansion. Nevertheless, they are equivalent for values close to 1 pu. This thesis uses a linearization based on Wirtinger's calculus. Like the previous linearization, this is equivalent for values close to 1 pu. However, the advantage of this approach is that it guarantees an affine separation between voltages and powers in the optimization model. The distributed resources are considered by using a ZIP model. A deep mathematical analysis of this linearization is beyond the objectives of this thesis, but it can be found in [D.A.Ramirez et al., 2019]. The approximated representation of a three phase grid-connected is given based on Equation (2.3). From this, the linearization is presented below in a complex matrix representation:

$$S^* = H \cdot V_N^* + M \cdot V_N + T \tag{3.5}$$

where H, M, T are constant matrices defined by:

$$H = \operatorname{diag}(Y_{Sk} \cdot V_S) + \operatorname{diag}(Y_N \cdot V_{N0}) \tag{3.6}$$
$$M = \operatorname{diag}(V_{N0}^*) \cdot Y_N \tag{3.7}$$
$$T = -\operatorname{diag}(V_{N0}) \cdot (Y_N \cdot V_{N0}^*) \tag{3.8}$$

Therefore, Equation (2.15) can be represented as follows:

$$(p_{kG} - p_{kD}) + j(q_{kG} - q_{kD}) = T_k + \sum_{m=1}^{N} H_{km} v_m^* + M_{km} v_m \tag{3.9}$$

Notice that (3.9) define an affine space, even when it is separated into real and imaginary parts, since neither H, M or T depends of the power as is the case of [Garces, 2016].

3.3 Stochastic model

The proposed model is designed for microgrids and small power distribution systems. Therefore, the irradiance scenario is the same for all the panels in the grid. The proposed methodology takes real data for generated power and define n_t scenarios with probability ξ_t (the generation of scenarios will be presented in the next section). In this situation, the expected value of the losses can be represented by the following sample average approximation which defines an affine equation:

$$\mathbb{E}(p_L, \xi_t) = \sum_{t}^{n_t} \xi_t p_{Lt} \tag{3.10}$$

where ξ_t is the probability of each scenario. The number of scenarios can grow very fast in many power systems applications. However, the main supposition of this work is that the solar panels are very close geographically and hence, the scenario is the same in all the panels along the microgrid. In this situation, the value of n_t is small as will be presented in the results. The radiation level is different every hour, with that in mind the generation of the system is going to change for each hour, allowing us to obtain different profiles of power factor for each hour.

3.4 Formulation of the convex model

For the sake of completeness, the convex model is presented below. This model include constrains from Model 1 that are already convex and the approximations presented before:

Model 2 *Convex model for the optimal set point of the reactive power in a three-phase microgrid:*

$$\min \sum_{t}^{n_t} \xi_t p_{Lt} \tag{3.11}$$

$$(p_{kG} - p_{kD}) + j(q_{kG} - q_{kD}) = T_k + \sum_{m=1}^{N} H_{km} v_m^* + M_{km} v_m \tag{3.12}$$

$$p_L \geq \sum_{k} \sum_{m} \text{real}(v_k^* y_{km} v_m) \tag{3.13}$$

$$v_{slack} = 1e^{j\phi} \tag{3.14}$$

$$v_{min} \leq \|v_k\| \leq v_{max} \tag{3.15}$$

$$\sqrt{p_{kG}^2 + q_{kG}^2} \leq s_{k(max)} \tag{3.16}$$

$$p_{kG} = p_{kG(max)}(\xi_t) \tag{3.17}$$

$$q_{kG} = \rho_k p_{kG} \tag{3.18}$$

The previous model allows us to obtain from the multiple solar radiation scenarios, a unique value of power factor for each of the installed generators, with this value of the power factor. Note this model is convex and tractable if the number of scenarios is finite. It is possible to calculate φ outside the model by using the magnitude of reactive power with which the converters must be configured, as follows:

$$\rho_k = \sqrt{(1/\varphi_k^2) - 1} \tag{3.19}$$

It is importat to remark that q_{kG}, v_k, p_L are variables that depends on the scenario. However, ρ_k is a decision variable that is independent of the scenario. This is a "here and now" variable.

3.5 Statistical scenarios

Real information of solar radiation is used to obtain several statistical scenarios. This data can be taken by the use of a pyranometer. Figure 3.2, presents the behavior of the solar radiation over the course of a month. The methodology to generate the multiple scenarios, it to calculate an histogram for each hours of the day. The information presented in these

histograms, are accumulated data of radiation and frequency of occurrence over a month at the same hour.

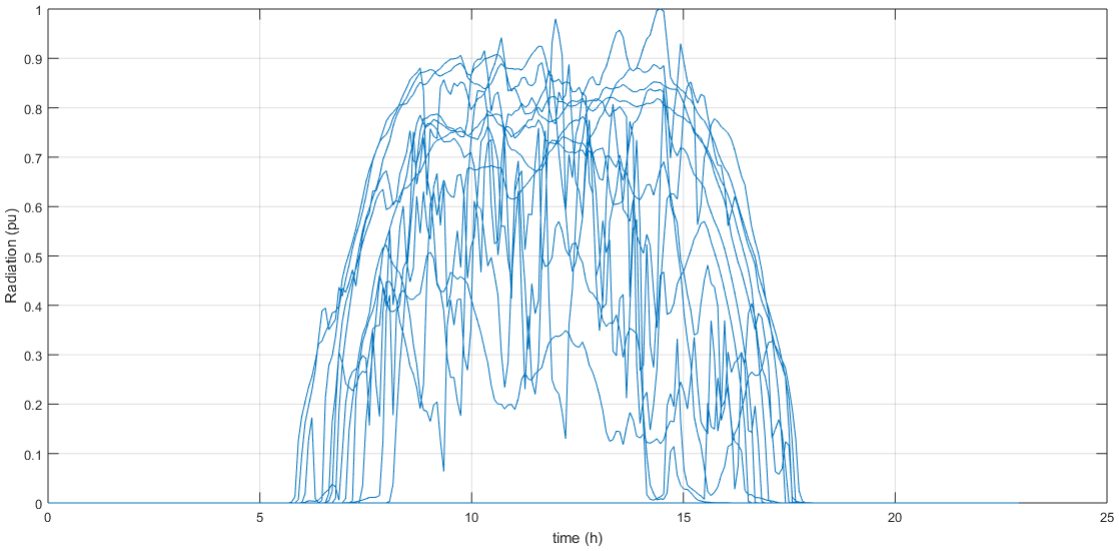

Figure 3.2: Radiation behaviour on a month

Chapter 4

Results

4.1 Test system and deterministic case

As an initial stage prior to the analyzes carried out with the stochastic model, it was performed a deterministic test on a modified version of the CIGRE benchmark test system for low voltage microgrids [Papathanassiou et al., 2005]. This test system is depicted in Figure 4.1. As the majority of low-voltage public distribution networks, it has a radial layout with the same conductors type and nodal distribution of presented on [Papathanassiou et al., 2005] but with some modifications. This modified microgrid have three single-phase solar-photovoltaic systems connected to each phase of the Node 6, 10 and 14 and one three-phase solar-photovoltaic system placed on Node 18. also it has six balanced loads located at Nodes 3, 8, 11, 14, 15 and 19.

Beside this the loads are changing in function of the load curve. It is assumed that all loads changes simultaneously with the same curve. Figure 4.2 shows the change in the magnitude of the load according to the time. This curve was created taking into account the typical day Colombian power systems where the peak is obtained at 20h and the valley at 3h.

The deterministic version of Model 2 was solved in CVX, a package for specifying and solving convex programs [Grant and Boyd, 2014]. Complex variables are allowed in CVX, therefore, its implementation is straitforward from Model 2 (the code is presented in Appendix C). The model is executed in a computer with the next settings: Intel(R) Pentium(R) Silver N5000 processor with 4 GB of RAM. Recall that in this case, the radiation and probability value would be defined in a punctual manner and not as a result of a statistical study as will be carried out later. For this deterministic test, it is assumed that at mid-morning (12

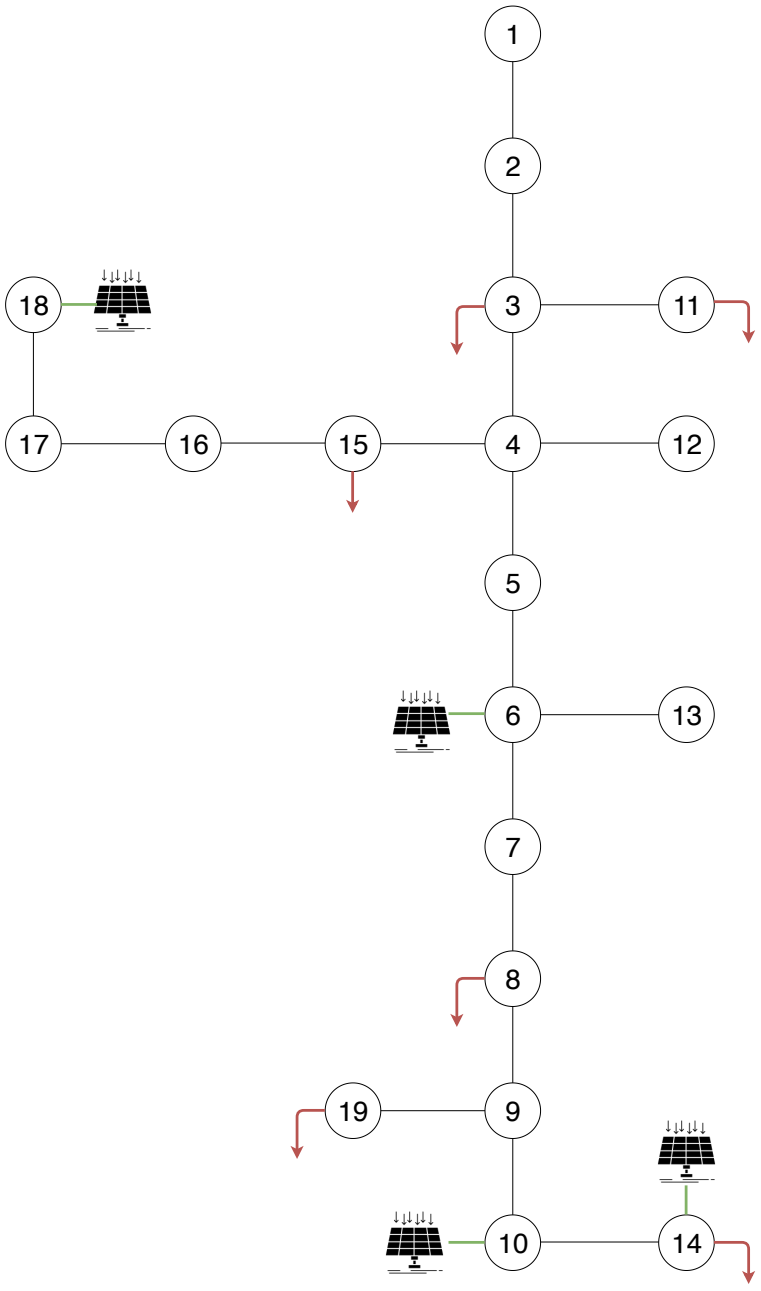

Figure 4.1: Nodal distribution and load/source placement through the microgrid

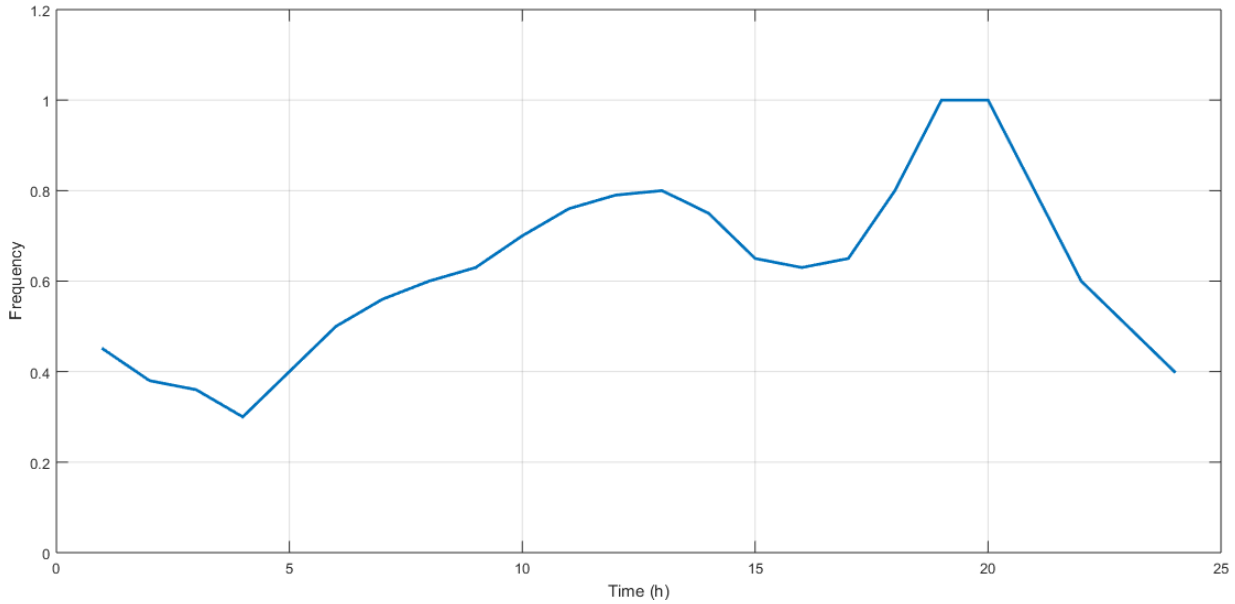

Figure 4.2: Load curve

p.m). The radiation value will be $1000W/m^2$ and a probability of occurrence of 100%. The solution for this deterministic case is presented in Table 4.1.

Table 4.1: Power factor solution for deterministic experimentation

Generator	Node	Phase	PF
1ϕ	6	A	0.9349
1ϕ	10	B	0.8333
1ϕ	14	C	0.8783
3ϕ	18	ABC	0.8895
Losses (pu)	1.1732		

The computational time for solving the model was 6.0330 seconds. The information presented on Table 4.1, shows that for this deterministic experimentation, which includes unbalanced phases on the generation and balanced loads, the optimal power factor is below of 1pu. Notice that a power factor below 1pu in a generation unit implies that the generation requires to inject reactive power to the grid.

4.2 Stochastic model

To obtain several solar scenarios, it was used information supplied by [(NREL), 2006] choosing the month of August of 2006 for a real solar plant located in Florida U.S.A. The information was taken on intervals of five minutes. In Appendix C, it is presented the code which allow us to process this radiation information and generate the scenarios. The code presented, allows the selection of the hour of the study (scenario), and choose the number of cases. The resulting information on the code, is used by each of the generators, single phase or three-phase connected to the grid, to change their active power magnitude through the time.

The stochastic phenomenon was modeled using Montecarlo Sample Method (MSM), using the methodology *Here and Now*, with the information described in Chapter 3. Using this database, ten cases of solar radiation were generated, for three specific hours at the day, one at sunrise it means at 7:00 a.m, the second one at mid-morning, which is at 9:00 a.m and the last one at maximum solar radiation point which is at 12:00 p.m. In each case, the frequency is used to estimate the probability of the scenario.

4.2.1 Case 1 at 7 a.m

The first case was evaluated at 7:00 a.m when the solar radiation is very low. The computational time was 8.7574 seconds. In this case, the radiation level is low and hece, the scenarios of low generation are higher as shown in Figure 4.3.

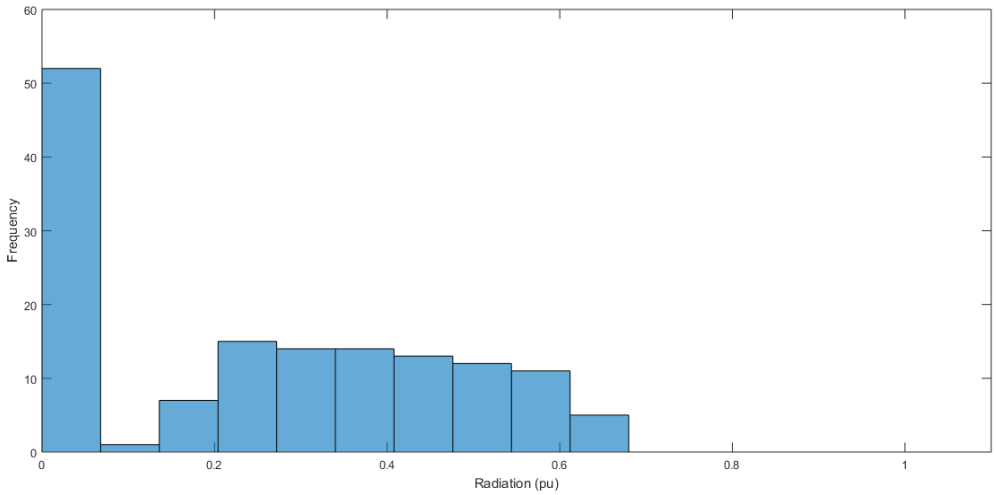

Figure 4.3: Radiation scenarios for 7 a.m.

Ten scenarios were considered although the method can be extended to any number of realizations. However, different simulations shown that this amount of scenarios was enough to demonstrate the performance of the method. Figure 4.4 shows the losses of the system after solving the stochastic optimization model, it can be seen that when the radiation level is low the losses are higher and when the radiation start to increase, the losses get reduced, that is because the sources supply power to the loads.

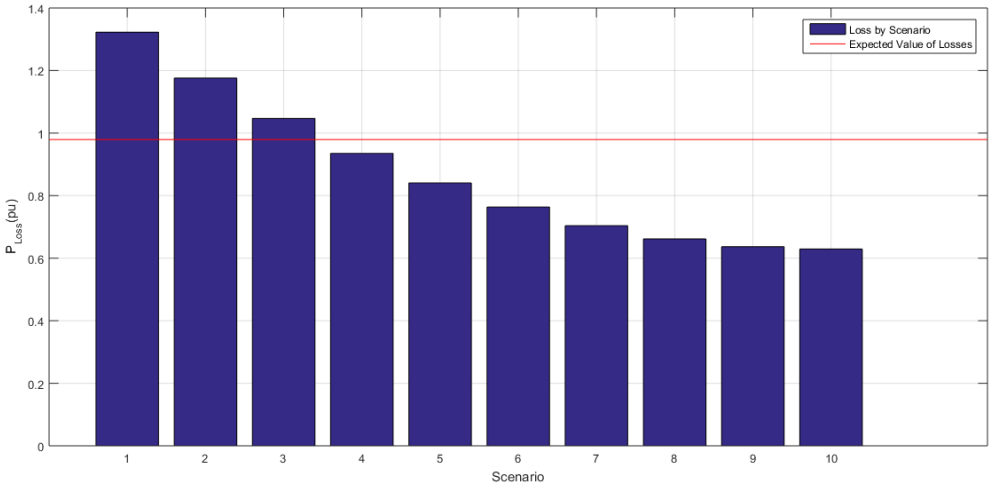

Figure 4.4: Losses on the system for the 7 a.m set of scenarios.

Table 4.2 presents the optimal power factor for each solar-photovoltaic unit as an outcome of the optimization problem. As expected, losses were higher for the scenarios of low solar radiation. However, in all these scenarios, the losses are improved by using the fixed value of power factor given in the table.

Table 4.2: Power factor for 7 a.m scenario

Generator	Node	Phase	PF
1ϕ	6	A	0.8412
1ϕ	10	B	0.7071
1ϕ	14	C	0.7574
3ϕ	18	ABC	0.7443
Expected Losses (pu)	0.9793		

4.2.2 Case 2 at 9 a.m

The second test was evaluated at 9:00 a.m or mid-morning with a computational time of 11.5907 seconds. The radiation level at this hour presents higher values than Case 1, as shown in Figure 4.5.

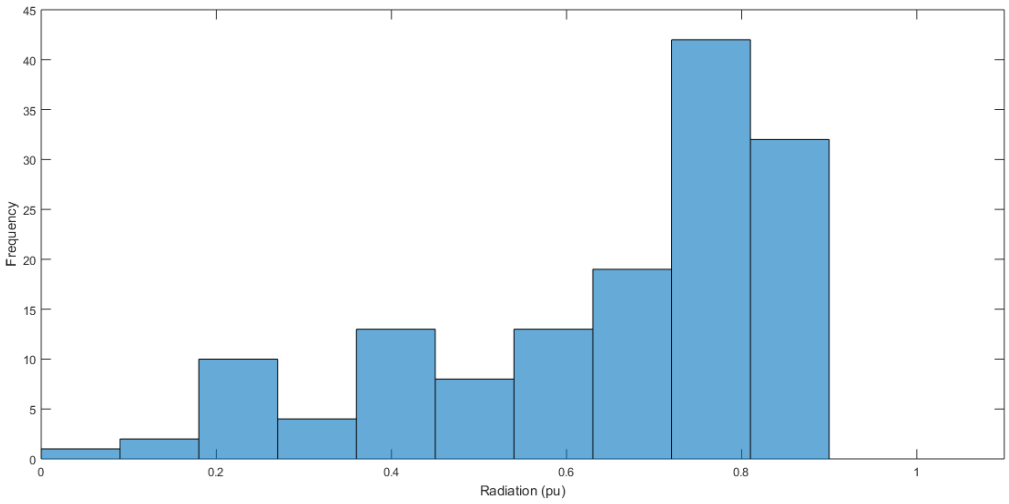

Figure 4.5: Radiation scenarios for 9 a.m

Figure 4.6 shows the losses of the system, it can be seen that when the radiation level is low the losses are higher and when the radiation start to increase, the losses get reduced, that is because the sources supply power to the loads.

Table 4.3 present the optimal power factor for each generator. It can be observed than the expected value of losses are lower than previous test due to the increasing on the solar irradiance.

Table 4.3: Power factor for 9 a.m scenario

Generator	Node	Phase	PF
1ϕ	6	A	0.9107
1ϕ	10	B	0.7474
1ϕ	14	C	0.8452
3ϕ	18	ABC	0.8818
Expected Losses (pu)	0.8574		

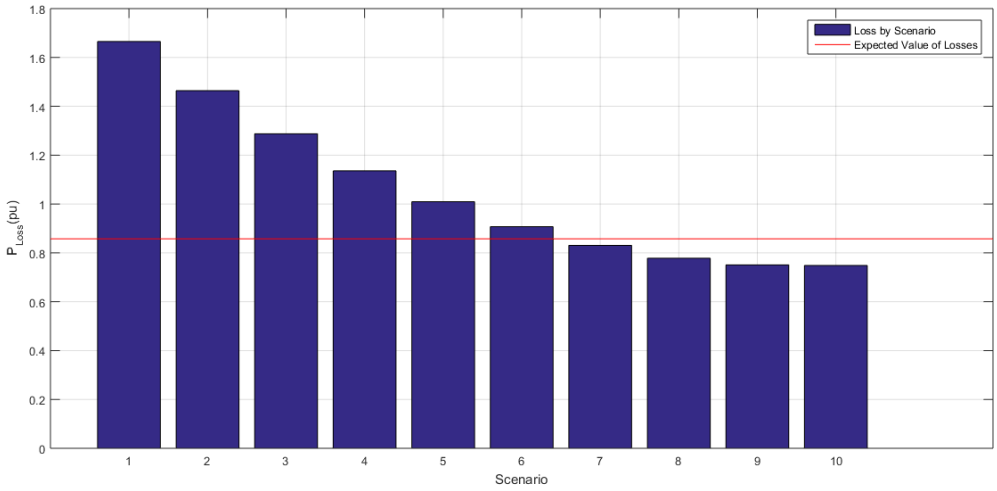

Figure 4.6: Losses on the system for the 9 a.m set of scenarios.

4.2.3 Case 3 at 12 p.m

This case was evaluated at 12:00 p.m with a computational time of 11.0697 seconds; at this time, the peak level of maximum solar radiation is found, higher than cases 1 and 2, as shown in Figure 4.7.

Figure 4.8, shows the losses of the system, it can be seen that when the radiation level is low the losses are higher and when the radiation start to increase, the losses get reduced, that is because the sources supply power to the loads.

Table 4.4 presents the optimal power factor for each generator as an outcome of the optimization problem. Besides it can be seen than the expected value of losses is higher than previous test, that is because higher load of the system. The slack node has to supply the loads recognizing that as losses of the system.

Table 4.4: Power factor for 12 p.m scenario

Generator	Node	Phase	PF
1ϕ	6	A	0.8731
1ϕ	10	B	0.7917
1ϕ	14	C	0.7967
3ϕ	18	ABC	0.7917
Expected Losses (pu)	1.5148		

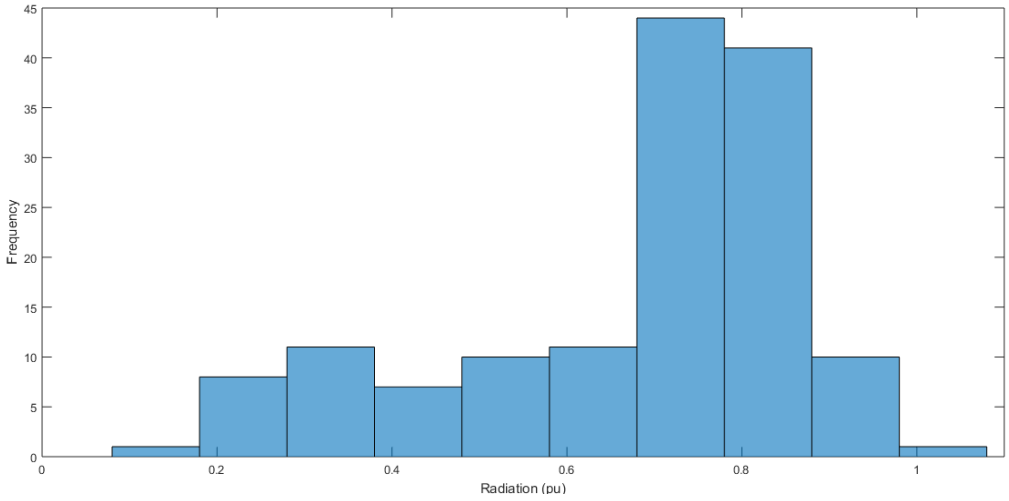

Figure 4.7: Radiation scenarios for 12 p.m

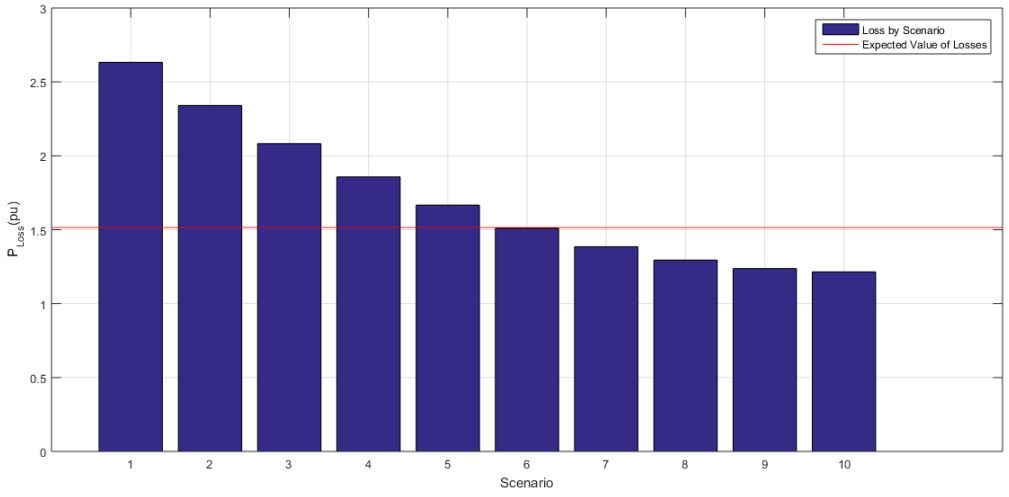

Figure 4.8: Losses on the system by scenario

4.3 Using the model for increasing hosting capacity

Taking into account the methodology for reactive power control developed on previous chapters and complementing the stochastic model with a constraint that limits the voltage of distribution lines setting its maximum to 1.1 pu. It is applied a hosting capacity model to analyse the behaviour of the optimization model on the high radiation hour (12 p.m). This scenario will be analyzed for 10 cases of solar radiation by hour which control the magnitude of active power that the photovoltaic sources inject to the grid. This hosting capacity model which is the same of the end of Chapter 3, takes into account different source and charge behaviours, with them is possible to find the maximum generation level that our grid can hold without violate the voltage level level set up before on the constraint. This value on the simulation process is called *Maximum Multiplication Factor* or MMT, this factor indicates the magnitude of active power that generation nodes can hold without break the voltage bound. Tables B.1 and B.2 given in Appendix B show two settings, one for balanced three phase loads, it means that active and reactive power are the same on each phase, and the second one display unbalanced loads where active and reactive power are different this information will be used on the multiple cases studied below.

4.3.1 Results for Balance Source - Balance Load (Bs-Bl)

On the development of this test, is used the generation information placed on Table B.3 and load values from Table B.1.

Table 4.5: Power factor and MMF for balanced source - balanced load

Generation Nodes	**Case 12 p.m**	
	Power factor	**Maximum multiplication factor (MMF)**
6	0.8868	1.9
10	0.7917	
14	0.9582	
18	0.9878	
Expected Value of Losses (pu)	0.8614	

The solution of this test presented on Table 4.5 shows the optimal setting of power factor for each generator, also is presented the maximum multiplication factor for this case.

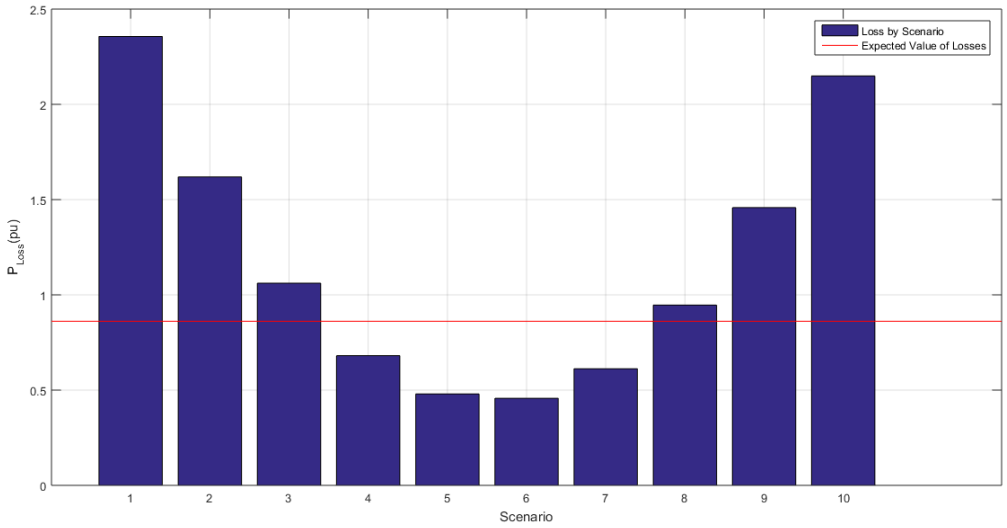

Figure 4.9: Losses of the system by scenario 12 p.m.

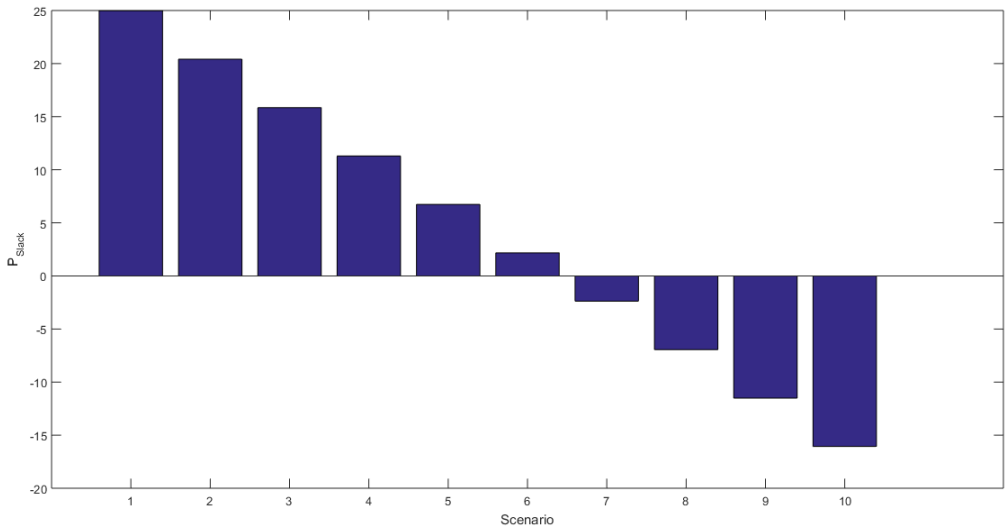

Figure 4.10: Power flow in slack node for balanced operation and increasing of the capacity.

Figure 4.9 present the losses on each of the 10 cases of radiation, we can be see in this figure that on low radiation levels the losses turn higher, that is because the power supplied by the solar sources are low and the slack node have to supply the power that the load

needs, but on high radiation levels, the power rise again, that situation happens when there is unused power provided for the sources, which flow back to the slack node. Figure 4.10 shows the power flow on the slack node, here can be observed the case when the power starts to flow back to the slack node.

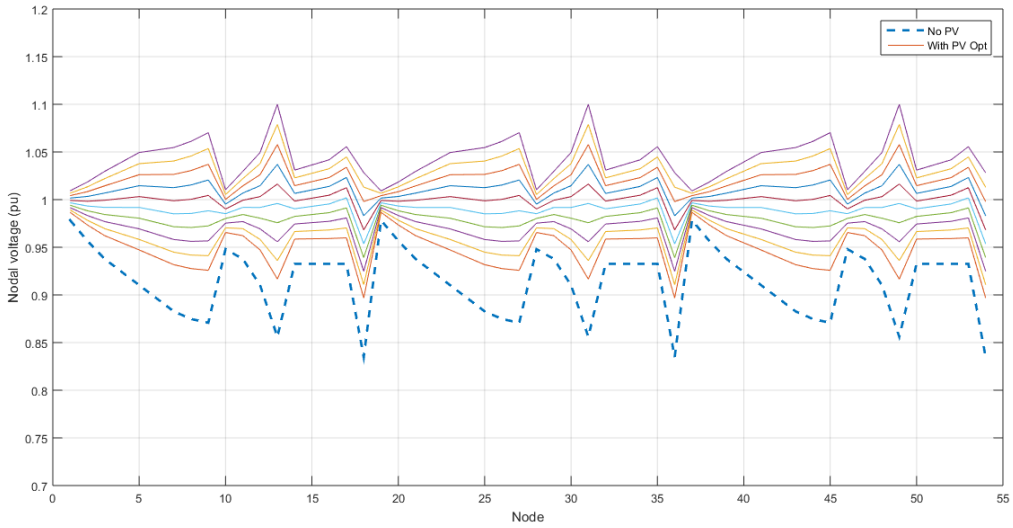

Figure 4.11: Nodal voltages

Figure 4.11 presents the nodal voltages of the 19 nodes system with the higher point of MMF, on this graphic, the nodal voltages are distributed on phase a, b and c. Beside this, it is observed that from the lowest levels of radiation, an improvement in the nodal tensions of around 0.5 pu is being seen in contrast with the system without any solar generator represented on the graphic as a dotted line.

4.3.2 Results for Balance Sources - Unbalance Loads (Bs-Ul)

On the development of this test, is used the generation information placed on Table B.3 and load values from Table B.2.

Table 4.6: Power factor and MMF for balanced source - unbalanced load

Generation Nodes	**Case 12 p.m**	
	Power factor	**Maximum multiplication factor (MMF)**
6	0.8237	1.7
10	0.7917	
14	0.9708	
18	0.9666	
Expected Value of Losses (pu)	1.1488	

The solution of this test presented on Table 4.6 shows the optimal setting of power factor for each generator, also is presented the maximum multiplication factor for this case.

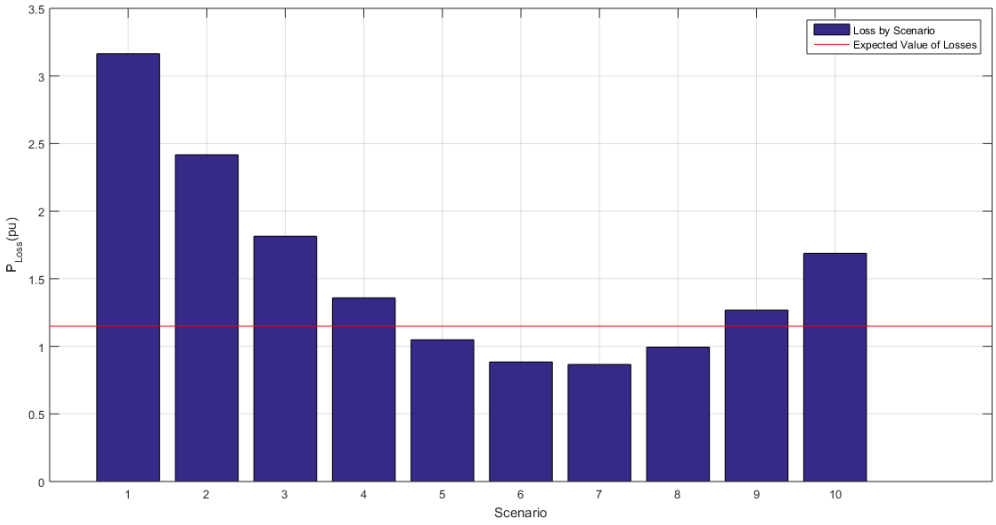

Figure 4.12: Losses of the system by scenario 12 p.m.

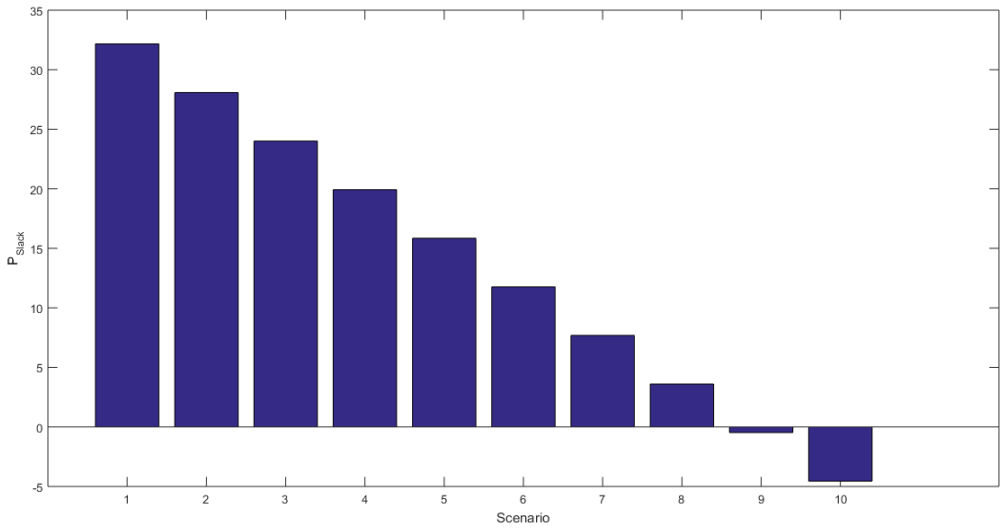

Figure 4.13: Power flow on slack node

Figure 4.12 present the losses on each of the 10 cases of radiation, we can be see in this figure that on low radiation levels the losses turn higher, that is because the power supplied by the solar sources are low and the slack node have to supply the power that the load needs, but on high radiation levels, the power rise again, that situation happens when there is unused power provided for the sources, which flow back to the slack node. Figure 4.13 shows the power flow on the slack node, here can be observed the case when the power starts to flow back to the slack node.

Figure 4.14 presents the nodal voltages of the 19 nodes system with the higher point of MMF, on this graphic, the nodal voltages are distributed on phase a, b and c. Beside this, it is observed that from the lowest levels of radiation, an improvement in the nodal tensions of around 0.5 pu is being seen in contrast with the system without any solar generator represented on the graphic as a dotted line.

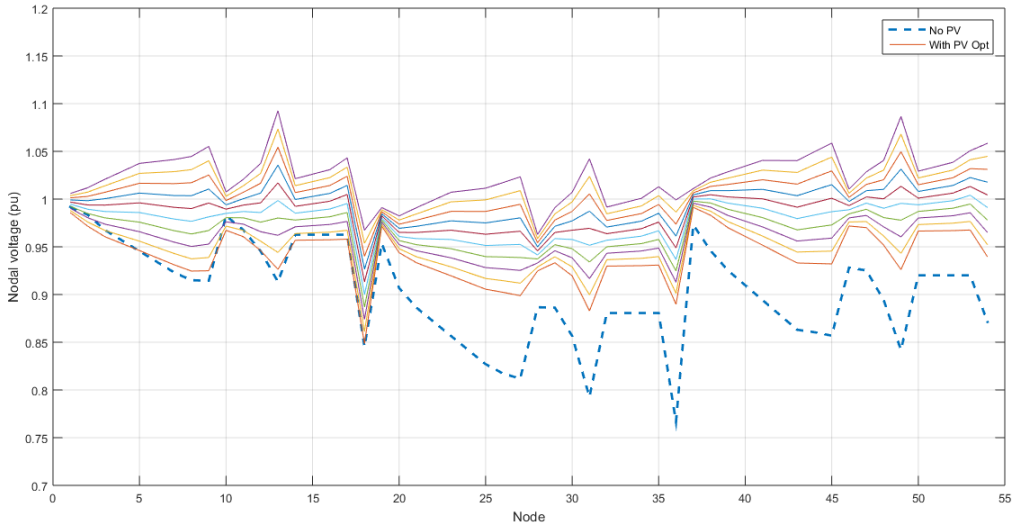

Figure 4.14: Nodal voltages

4.3.3 Results for Unbalance Source - Balance Load (Us-Bl)

On the development of this test, is used the generation information placed on Table B.4 and load values from Table B.1.

Table 4.7: Power factor and MMF for unbalanced source - balanced load

Generation Nodes	**Case 12 p.m**	
	Power factor	**Maximum multiplication factor (MMF)**
6	0.9621	2.3
10	0.8903	
14	0.8070	
18	0.9436	
Expected Value of Losses (pu)	1.6450	

The solution of this test presented on Table 4.7 shows the optimal setting of power factor for each generator, also is presented the maximum multiplication factor for this case. Can be observed that on situations where the generation is unbalanced, the expected value of losses become higher.

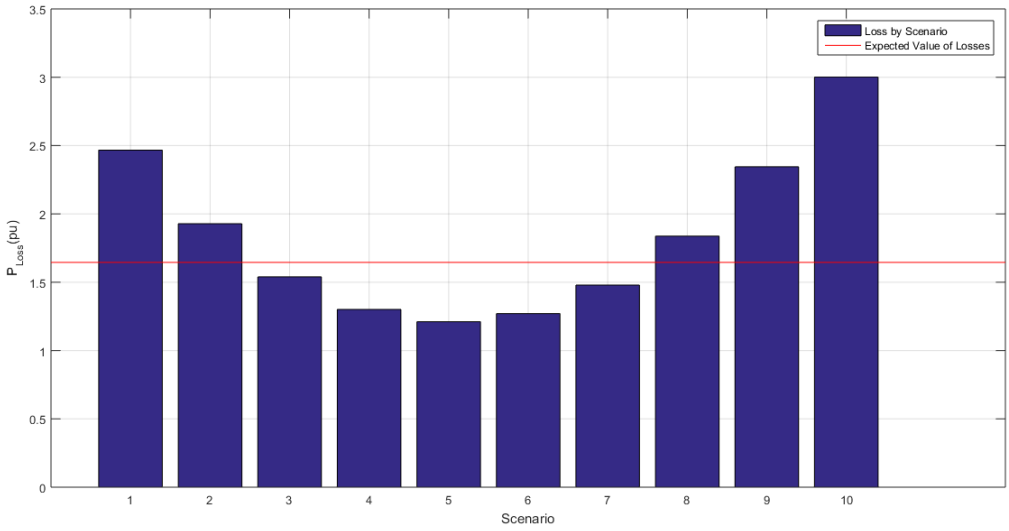

Figure 4.15: Losses of the system by scenario 12 p.m.

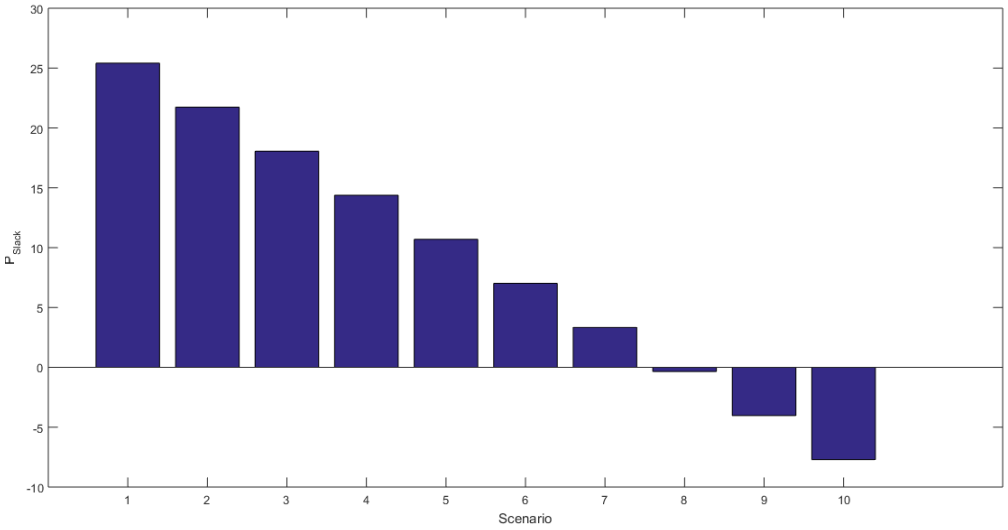

Figure 4.16: Power flow on slack node

Figure 4.15 present the losses on each of the 10 cases of radiation, we can be see in this figure that on low radiation levels the losses turn higher, that is because the power supplied by the solar sources are low and the slack node have to supply the power that the load

needs, but on high radiation levels, the power rise again, that situation happens when there is unused power provided for the sources, which flow back to the slack node. Figure 4.16 shows the power flow on the slack node, here can be observed the case when the power starts to flow back to the slack node.

Figure 4.17 presents the nodal voltages of the 19 nodes system with the higher point of MMF, on this graphic, the nodal voltages are distributed on phase a, b and c. Beside this, it is observed that from the lowest levels of radiation, an improvement in the nodal tensions of around 0.5 pu is being seen in contrast with the system without any solar generator represented on the graphic as a dotted line.

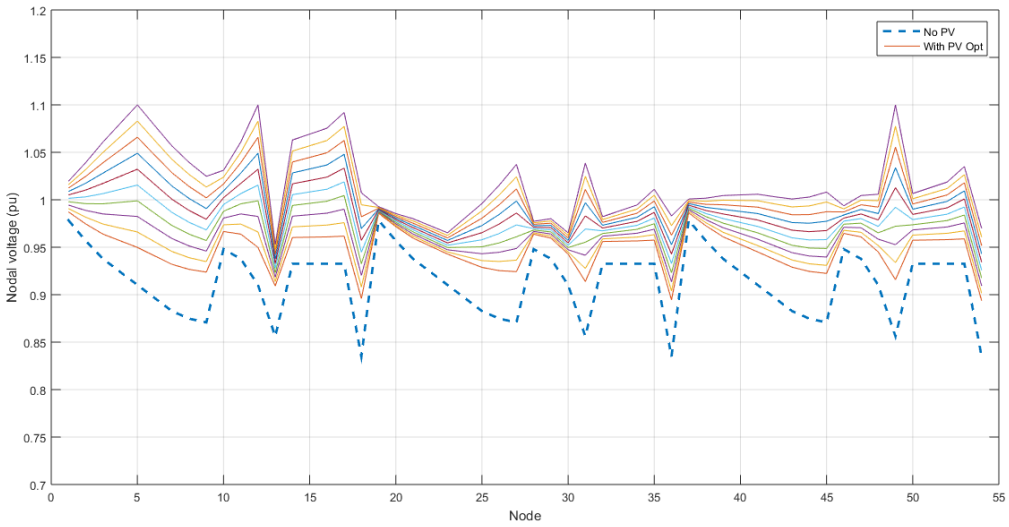

Figure 4.17: Nodal voltages

4.3.4 Results for Unbalance Source - Unbalance Load (Us-Ul)

On the development of this test, is used the generation information placed on Table B.4 and load values from Table B.2.

Table 4.8: Power factor and MMF for unbalanced source - balanced load

Generation Nodes	**Case 12 p.m**	
	Power factor	**Maximum multiplication factor (MMF)**
6	0.9831	2.3
10	0.9220	
14	0.7917	
18	0.8685	
Expected Value of Losses (pu)	2.1822	

The solution of this test presented on Table 4.8 shows the optimal setting of power factor for each generator, also is presented the maximum multiplication factor. Can be observed that on situations where the generation is unbalanced, the expected value of losses become higher.

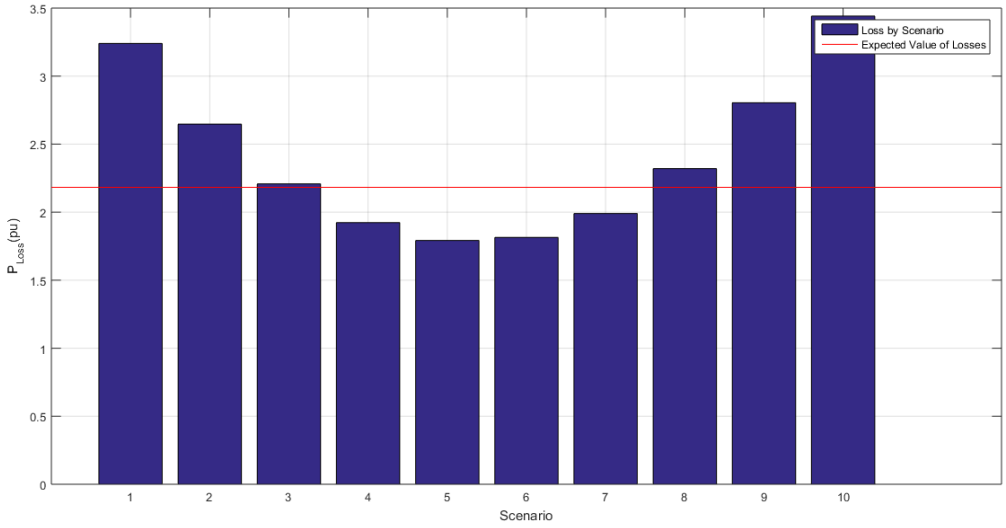

Figure 4.18: Losses of the system by scenario 12 p.m.

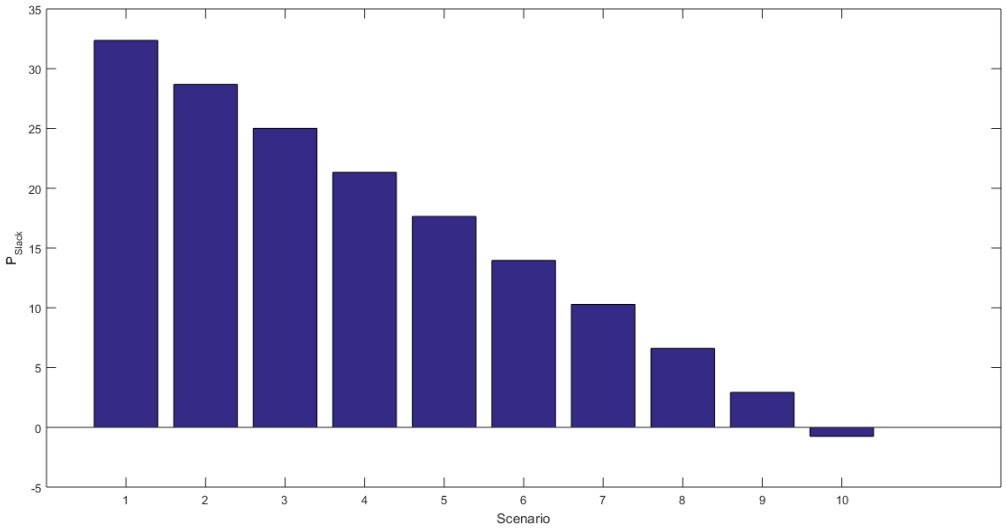

Figure 4.19: Power flow on slack node

Figure 4.18 present the losses on each of the 10 cases of radiation, we can be see in this figure that on low radiation levels the losses turn higher, that is because the power supplied by the solar sources are low and the slack node have to supply the power that the load needs, but on high radiation levels, the power rise again, that situation happens when there is unused power provided for the sources, which flow back to the slack node. Figure 4.19 shows the power flow on the slack node, here can be observed the case when the power starts to flow back to the slack node.

Figure 4.20 presents the nodal voltages of the 19 nodes system with the higher point of MMF, on this graphic, the nodal voltages are distributed on phase a, b and c. Beside this, it is observed that from the lowest levels of radiation, an improvement in the nodal tensions of around 0.5 pu is being seen in contrast with the system without any solar generator represented on the graphic as a dotted line.

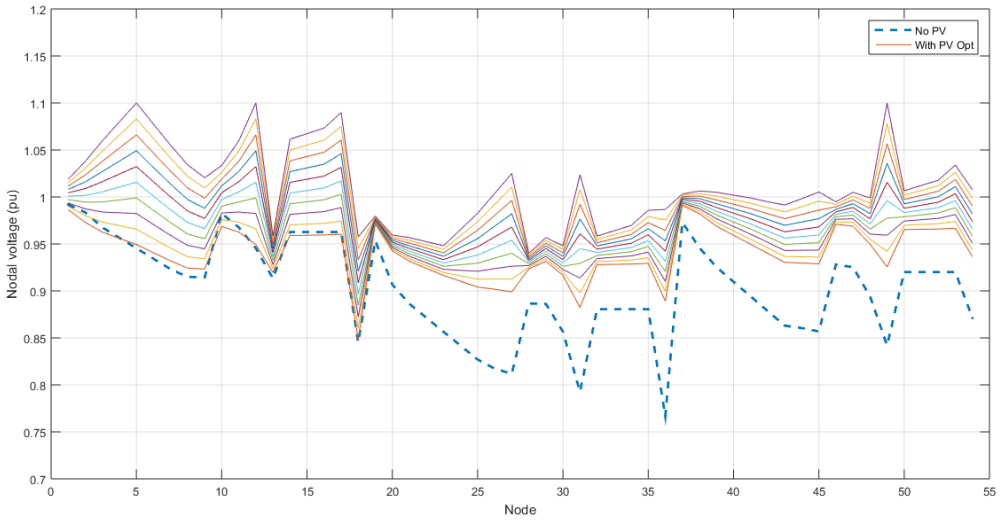

Figure 4.20: Nodal voltages

4.3.5 Results for system without power factor control

To verify the effectiveness of the model described in previous chapters and its effect in terms of the improvement of the hosting capability of the network, a test was executed with the same parameters used in the case of balanced loads/balanced sources, in addition to this, the value of MMF is configured to the same value presented on that test and finally, deactivating in the applied stochastic model, the ability to control the reactive power and thereby force the system to operate with unit power factor. The table 4.9, shows the obtained results for this test.

Table 4.9: Power factor and MMF for Bl-Bl (no reactive power control)

Generation Nodes	**Case 12 p.m**	
	Power factor	**Maximum multiplication factor (MMF)**
6	1	1.9
10	1	
14	1	
18	1	
Expected Value of Losses (pu)	1.6745	

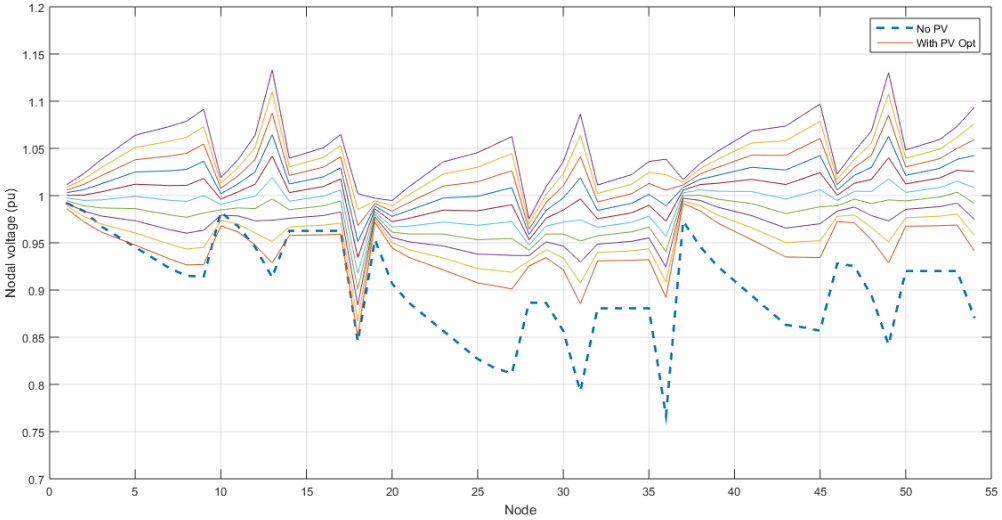

Figure 4.21: Nodal voltages

It is observed that in contrast to the test whose reactive control restrictions are activated, that the losses of the system become higher, Figure 4.22 and the expected value of the losses is around double, also it is noted in Figure 4.21, that the voltage magnitude increases above the physical limitation described on the restrictions, so the effectiveness of the model to improve network quality is seen. Finally, the power supplied by the slack node become higher even on high radiation levels, being this a factor that influence the increase on losses described above, Figure 4.23

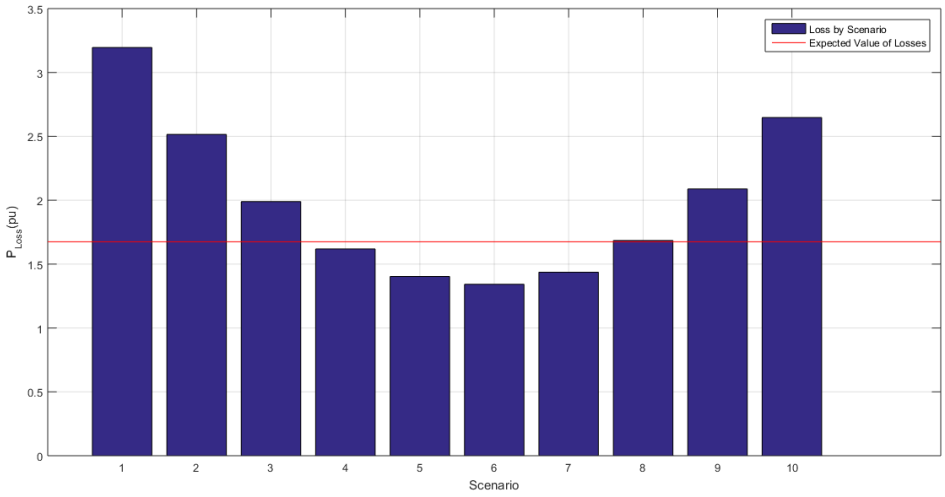

Figure 4.22: Losses of the system by scenario 12 p.m.

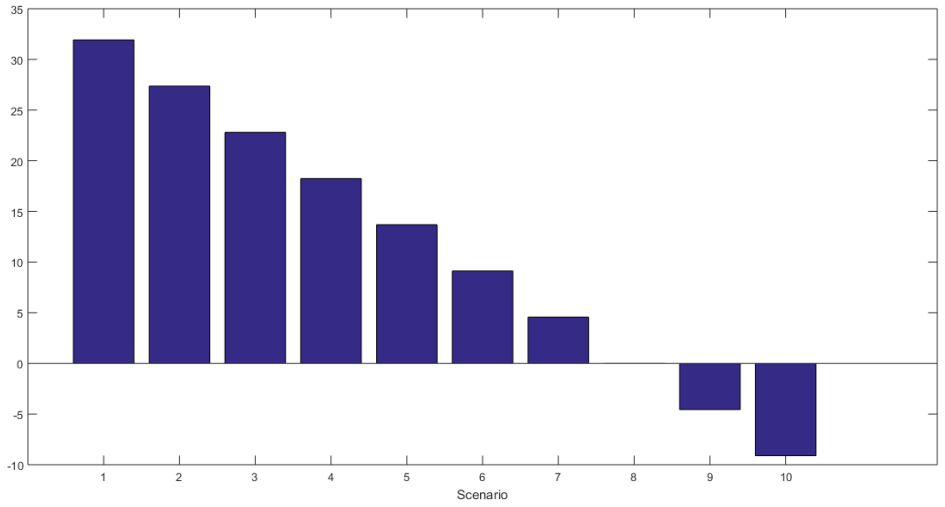

Figure 4.23: Power flow on slack node

Chapter 5

Conclusions

The development of an alternative methodology for reactive power management on microgrids was presented, this allows through the use of linearized models, stochastic analysis and convex optimization, control reactive power on the grid. The reactive power control can be done, taking advantage of the solar converters capability to inject or consume reactive power manipulating the switching of its electronic components (IGBT's).

Based on our study, from low to high levels of radiation, the proposed methodology allows to conclude that as the radiation level increase, the active power increase too, resulting on an unwanted rise of voltage which tends to be mitigated by the system sources injecting reactive power. Normally, control voltage rises on networks is done by the use of reactive compensating devices, for which our methodology is presented as a possible solution to replace those devices.

According to the numeric and graphic results, the lower value of losses are presented at 9 am scenario, in a nutshell, when there are surpluses of active power, like on 12 pm scenario, where the solar panels operate at maximum, if that power is not consumed by the loads, the losses tend to increase due a flow back of unused active power to the slack node.

The use of stochastic analysis, allows across the use of real solar radiation develop precise predictions of possible radiation states. The use of precise prediction applied on the proposed methodology, allow to set effectively the power factor behavior on the sources for an operation throughout the day, all year without the need of a master controller which could increase the operation cost of a microgrid.

A derived benefit product of the investigation, is to give to distributed systems with distributed energy resources (DER's), the ability to increase its hosting capacity, which allows to the system, hold higher generation magnitudes on the grid, without break design constraints, avoiding voltage increments reducing the risk of voltage increments on nodes.

The results show that if many generators are installed or accumulated on consecutive nodes, the hosting capacity of the grid is reduced due dangerously high voltage increments because of high levels of active power. The ideal is distribute in a balanced way the energy resources among all the system nodes, being the ideal generators three-phase, that is because it allows include more generators than single-phase ones.

5.1 Future Research

As future work, it is proposed to perform extensions on the mathematical and stochastic model, that is, include energy storage such as batteries or flywheels, adding charging and discharging restrictions. Apply this optimization model on complex grid designs. Finally, add the stochastic wind speed behavior to include wind generators to the system.

Appendix A

Three phase network modelling

When it is desired to perform a study that involves power systems, in this case applied to three-phase networks with multiple elements such as generators, loads, transformers and transmission lines, it is essential to model the parameters that constitute these elements and the interaction of these with the different nodes of the system.

The formulation of a mathematical model is considered the first stage for the study of electrical networks. The matrices are the fundamental tool for this modeling, since these allow us to perform large operations with large systems using digital computing systems, these network matrices are created using the independent characteristics of the elements and arrange them in such a way that they relate the nodes or points of connection to which they are connected. For our purposes, the main element that will be used is the Y-bus matrix. This element will be explained in the section above.

A.1 Y-bus matrix formulation

Normally, the representations of transmission or distribution systems tend to be done in single line illustrations, with the aim of reducing the saturation of the graphics due to the multiple lines that exist in real world. Figure A.1, shows a section of a transmission line from its connection with the busbar or node. although the illustration is represented as single line, we can observe that it is constituted by three phases (A, B, and C) and that for each of these, there is a current flow and an associated nodal voltage in addition to the admittances of the lines and the parallel admittances.

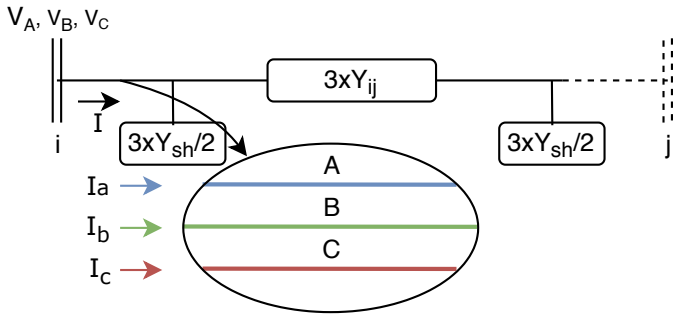

Figure A.1: Single Phase Representation of a Three-Phase System

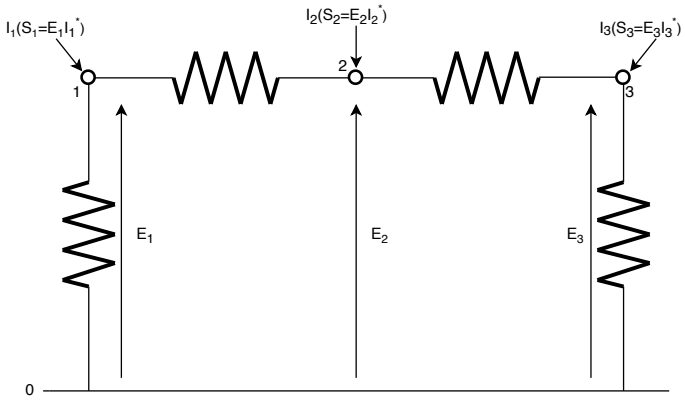

Figure A.2: Simple Network with Nodal Quantities

The Y-bus is constituted by all the elements previously mentioned. A three-phase modelling requires a Y-bus of size $3n \times 3n$

This tool is useful on application of iterative load flow analysis such as those based on Newton-Raphson, which are quite useful due to the little memory space they require, however, the disadvantage is that it takes long time to converge or in some cases never converge. The Y-bus matrix is presented as the initial stage of all these methods that is because it is the description of the state of the system components. Figure A.2 presents a single-line system with four nodes, for which we will develop the Y-bus matrix. The methodology for obtaining the admittance matrix for this system can be expanded to a three-phase system.

To perform nodal analysis, it is convenient to use the admittance of the lines instead

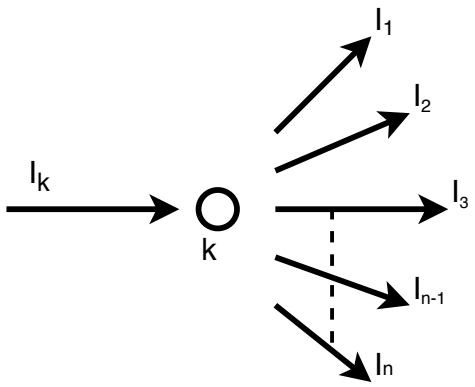

Figure A.3: First Kirchhoff Law Representation

of the impedance. The sending and receiving nodes are denoted as k and i, respectively. The admittance of the lines are denoted as y_{ki} and nodal voltages are denoted as E_k and E_i. [Arrillaga and Harker, 1983]. Being the current that flows from k to i denoted by:

$$I_k = y_{ki}(E_k - E_i) \tag{A.1}$$

The Kirchhoff's current law indicates that the injected current I_k, must be equal to the sum of currents leaving the k node. (See Figure A.3).

For the system presented on Figure A.2, this equation is shown as follows:

$$I_k = \sum_{i=0}^{n} y_{ki}(E_k - E_i) \tag{A.2}$$

since $E_0 = 0$, and the system is linear:

$$I_k = \sum_{i=0\neq k}^{n} y_{ki}(E_k) - \sum_{i=1\neq k}^{n} y_{ki}(E_i) \tag{A.3}$$

Expanding this equation on all the nodes of an electrical system, and organizing in function of the busbar numeration, we obtain the matrix form of the network:

Where, the self-admittance of node k is represented as:

$$Y_{kk} = \sum_{i=0\neq k}^{n} y_{ki} \tag{A.4}$$

Table A.1: Structure of a Y-bus for an n x n network

$$\begin{bmatrix} I_1 \\ I_2 \\ \vdots \\ I_n \end{bmatrix} = \begin{bmatrix} y_{11} & y_{12} & \dots & y_{1n} \\ y_{21} & y_{22} & \dots & y_{2n} \\ \vdots & \vdots & \vdots & \vdots \\ y_{n1} & y_{n2} & \dots & Y_{nn} \end{bmatrix} \begin{bmatrix} E_1 \\ E_2 \\ \vdots \\ E_n \end{bmatrix}$$

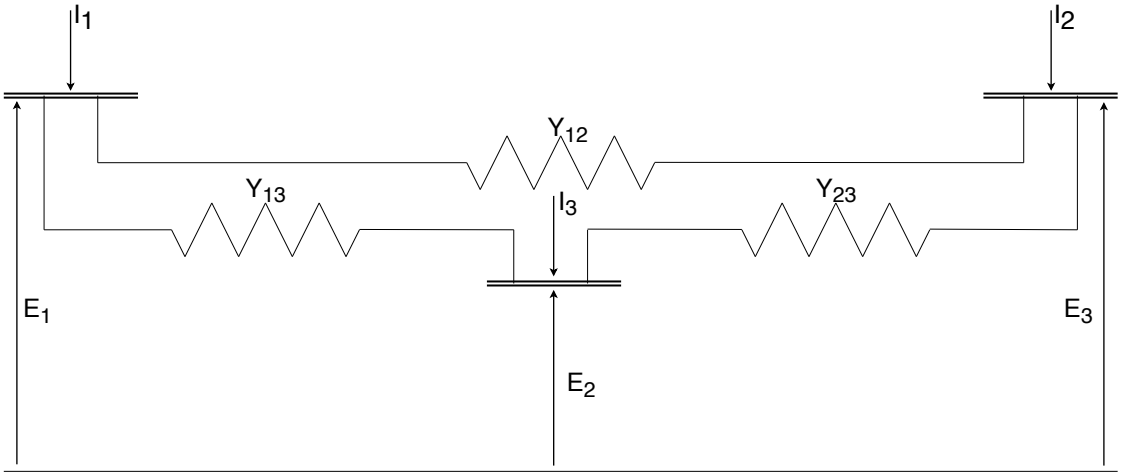

Figure A.4: Multi-nodal Example Grid

And the mutual admittance between nodes k and i is:

$$Y_{ki} = -y_{ki} \tag{A.5}$$

The information presented on Table 2.1 is the basic representation of the Y-bus for a system with a few nodes, Figure A.4 presents an example of a grid with multiple transmission lines connected to each node, for which the respective Y-bus obtained using Equations (A.4) and (A.5).

The Y-bus presented both Table A.1 and Table A.2 and in almost all the admittance matrix, have the next properties:

Table A.2: Admittance Matrix for System of Figure 2.4

$$\begin{bmatrix} I_1 \\ I_2 \\ I_3 \end{bmatrix} = \begin{bmatrix} y_{12} + y_{13} & -y_{12} & -y_{13} \\ -y_{21} & y_{12} + y_{23} & -y_{23} \\ -y_{31} & -y_{32} & y_{13} + y_{23} \end{bmatrix} * \begin{bmatrix} E_1 \\ E_2 \\ E_3 \end{bmatrix}$$

Table A.3: Three phase Y-bus order

$$Y_{bus} = \begin{array}{c|ccc} & \text{A} & \text{B} & \text{C} \\ \hline \text{A} & & & \\ \text{B} & & & \\ \text{C} & & & \end{array}$$

- Square of order **n** x **n**.
- The matrix is symmetrical, y_{ki}=y_{ik}.
- It allows the use of complex numbers.
- Matrix highly sparsed, because on large systems only a few mutual admittances exist.

The representations above shows an admittance matrix for single line systems. This investigation is going to work with three-phase systems, which Y-bus representation have to be thee-phase too, next will be show the phase order on the admittance matrix applied on the development of this thesis project.

Appendix B

System description

Here is presented the information of transmission lines that models the CIGRE benchmark.

Table B.1: Balanced loads of the grid

Node	Phase A	Phase B	Phase C
3	10000+5000i	10000+5000i	10000+5000i
8	30000+15000i	30000+15000i	30000+15000i
11	5000+2500i	5000+2500i	5000+2500i
14	20000+10000i	20000+10000i	20000+10000i
15	30000+10000i	30000+10000i	30000+10000i
19	20000+10000i	20000+10000i	20000+10000i

Table B.2: Unbalanced loads of the grid

Node	Phase A	Phase B	Phase C
3	10000+5000i	70000+45000i	30000+15000i
8	30000+15000i	30000+15000i	50000+18000i
11	5000+2500i	9000+4500i	8000+3500i
14	10000+6000i	20000+9000i	17000+10000i
15	30000+10000i	30000+10000i	30000+10000i
19	28000+10000i	18000+10000i	8000+3000i

Table B.3: Generation nodes and power capacity for Balanced source

Generator Node	Capacity (kW)	Type of Source
6	55	Three Phase
10	25	Three Phase
14	30	Three Phase
18	50	Three Phase

Table B.4: Generation nodes and power capacity for unbalanced source

Generator Node	Capacity (kW)	Type of Source
6	55	Phase B
10	25	Phase C
14	30	Three Phase
18	50	Three Phase

Table B.5: Node distributions of the CIGRE benchmark

N1	**N2**	**L(m)**	**type**
1	2	35	1
2	3	35	1
3	4	35	1
4	5	35	1
5	6	35	1
6	7	35	1
7	8	35	1
8	9	35	1
9	10	35	1
3	11	30	2
4	12	30	3
6	13	30	4
10	14	30	3
4	15	35	1
15	16	35	1
16	17	35	1
17	18	30	5
9	19	30	2

Table B.6: Distributed lines parameters

Rph	**Xph**	**Ro**	**Xo(ohm/km)**	**Cap(uF/km)**	**Conductor type**
0.284	0.083	1.136	0.417	0.38	(1) OL - Twisted cable 4x120 mm2 Al
3.690	0.094	13.64	0.472	0.05	(2) SC - 4x6 mm2 Cu
1.380	0.082	5.520	0.418	0.18	(3) SC - 4x16 mm2 Cu
0.871	0.081	3.480	0.409	0.22	(4) SC - 4x25 mm2 Cu
0.822	0.077	2.04	0.421	0.27	(5) SC - 3x50 mm2 Al + 35 mm2 Cu

Appendix C

Thesis codes

Code for scenario generation:

```
function Esc = GenerarEscenarios(Casos,hora);
load LosDatos  % Data, Dia, Hora, Rad
Rad = Rad/max(Rad);
NumT = length(Hora);
figure(1)
plot(tt*23,Rad)
grid on
xlabel('time (h)')
ylabel('Radiation (pu)')
grid on
a = find(Hora==hora);
N = Rad(a);
figure(2);
his = histogram(N,Casos);
xlim([0 1.1])
xlabel('Radiation (pu)')
ylabel('Frequency')
Freq = his.Values/length(N);
Marca = his.BinWidth*(1:Casos)-his.BinWidth/2;
Esc.Prob = Freq';
Esc.Radiacion = Marca';
```

Code for the CIGRE system description

```
function MicroGrid = CIGRE_MICROGRID;
%% CIGRE MICROGRID BENCHMARK
Vnom = 400;       % Voltage line to line in Volts
wnom = 2*pi*60;   % Nominal frequency
Snom= 10e3;

        % N1 N2 L(m) type
Lines  = [ 1   2   35 1 %
           2   3   35 1
           3   4   35 1
           4   5   35 1
           5   6   35 1 %
           6   7   35 1
           7   8   35 1
           8   9   35 1
           9   10  35 1 %
           3   11  30 2
           4   12  30 3
           6   13  30 4
           10  14  30 3  %
           4   15  35 1
           15  16  35 1
           16  17  35 1
           17  18  30 5
           9   19  30 2];
         % Rph  Xph  Ro  Xo(ohm/km)  Cap(uF/km)
Impedances = [0.284  0.083  1.136  0.417   0.38  % (1) OL - Twisted cable 4
    x120 mm2 Al
              3.690  0.094  13.64  0.472   0.05  % (2) SC - 4x6 mm2 Cu
              1.380  0.082  5.520  0.418   0.18  % (3) SC - 4x16 mm2 Cu
              0.871  0.081  3.480  0.409   0.22  % (4) SC - 4x25 mm2 Cu
              0.822  0.077  2.04   0.421   0.27];% (5) SC - 3x50 mm2 Al + 35
                  mm2 Cu

%  end

%Generacion Balanceada
             % NODO   % FASE  % Smax
% Converters = [  6        4        75E3
%                 10       4        25E3
%                 14       4        90E3
%                 18       4        50E3];

```

```
%Carga balanceada
NodalPower =[3   0   -10000-5000i      -10000-5000i      -10000-5000i
             8   0   -30000-15000i     -30000-15000i     -30000-15000i
             11  0    -5000-2500i       -5000-2500i       -5000-2500i
             14  0   -20000-10000i     -20000-10000i     -20000-10000i
             15  0   -30000-10000i     -30000-10000i     -30000-10000i
            19   0   -20000-10000i     -20000-10000i     -20000-10000i   ];


                % Organizar la estructura
NumN = max([max(Lines(:,1)),max(Lines(:,2))]);
NumL = length(Lines(:,1));
NumZ = length(Impedances(:,1));
for k = 1:NumL
    ty = Lines(k,4);
    long = Lines(k,3)/1000;
   z1 = Impedances(ty,1)+j*Impedances(ty,2);
   zo = Impedances(ty,3)+j*Impedances(ty,4);
   zs = (zo+2*z1)/3;
   zm = (zo-z1)/3;
   Z(:,:,k) = [zs,zm,zm;zm,zs,zm;zm,zm,zs]*long;
    B(:,:,k) = Impedances(ty,5)*wnom*long*1E-6*eye(3)/2;
end

Ybust = zeros(NumN*3);
for k = 1:NumL
    N1 = Lines(k,1);
    N2 = Lines(k,2);
  Ykm = inv(Z(:,:,k));
    Bf = B(:,:,k)*i;
    kN1 = [N1,N1+NumN,N1+2*NumN];
    kN2 = [N2,N2+NumN,N2+2*NumN];
    Ybust(kN1,kN1)=Ybust(kN1,kN1)+Ykm+Bf;
    Ybust(kN1,kN2)=Ybust(kN1,kN2)-Ykm;
    Ybust(kN2,kN1)=Ybust(kN2,kN1)-Ykm;
    Ybust(kN2,kN2)=Ybust(kN2,kN2)+Ykm+Bf;
end
MicroGrid.Vll   = Vnom;
MicroGrid.wnom  = wnom;
MicroGrid.Sbase = 10E3;
MicroGrid.NumN  = NumN;
MicroGrid.NumL  = NumL;
[rows col]=size(NodalPower);
MicroGrid.NumC  = rows;
```

```
86      MicroGrid.Lines = Lines;
87      MicroGrid.Impedances = Impedances;
88      MicroGrid.NodalPower = NodalPower;
89      MicroGrid.Ybust = Ybust;
90      MicroGrid.Converters= Converters;
91      MicroGrid.NumS = length(Converters(:,1));
92      MicroGrid.Snom=Snom;
```

Code for optimal power flow (OPF)

```
%% Flujo de carga en micro-redes
clc
clear all
NumEsc = 10;
hora = 12;
tic
curva_demanda = [0.45, 0.38, 0.36,0.30,0.40,0.5,0.56, 0.60, 0.63, 0.70,
    0.76, 0.79, 0.80, 0.75, 0.65,0.63, 0.65, 0.80, 1, 1,0.80, 0.60, 0.50,
    0.4];
MG = CIGRE_MICROGRID;
MG.NodalPower(:,3:5) = MG.NodalPower(:,3:5)*curva_demanda(hora);
Res = Flujo_MicroRed(MG);
Esc = GenerarEscenarios(NumEsc,hora);

%% Poner en por unidad
Vnom = MG.Vll/sqrt(3);
Snom= MG.Snom;
Zbase = Vnom^2/Snom;
MG.Ybust = MG.Ybust*Zbase;

%% Linealizacion
s = [1,MG.NumN+1,2*MG.NumN+1]; % Nodos Slack
Ns = setdiff(1:(3*MG.NumN),s);  % Los que no son slack
YN0 = MG.Ybust(Ns,s); %matriz nodos slack
YNN = MG.Ybust(Ns,Ns); %matriz nodos no slack
Y00= MG.Ybust(s,s);
Vflujo = Res.V(Ns)/Vnom;


% Tensiones nodo slack
V0a= [(1 + 0*i)];
V0b= [(-0.5 - 0.8660*i)];
V0c= [(-0.5 + 0.8660*i)];
v0= [V0a; V0b; V0c];

% Cargas
S = zeros(3*MG.NumN);
for k = 1:MG.NumC
    n = MG.NodalPower(k,1) ;% nodo
    S(n) = MG.NodalPower(k,3); % fase A
    S(n+MG.NumN) = MG.NodalPower(k,4); % fase B
    S(n+2*MG.NumN) = MG.NodalPower(k,5); % fase C
end
```

```
42    Spn = conj(S(Ns)'/Snom);
43    %% ELEMENTOS LINEALIZACION WIRTINGUER (Diego Alejandro)
44
45    t=[1; exp(-(i*2*pi)/3); exp((i*2*pi)/3)];
46    Vn0= kron(t,ones(n-1,1));
47    H= diag(YN0*v0) + diag(YNN*Vn0);
48    M= diag(conj(Vn0))*YNN;
49    T= -diag(Vn0)*(YNN*conj(Vn0));
50
51    %% Optimizacion de las Perdidas
52    DG = zeros(3*MG.NumN,MG.NumS);
53    Smax = MG.Converters(:,3)/Snom;
54          % Radiacion (1=Nom)    Probabilidad
55
56    for k = 1:MG.NumS
57        n = MG.Converters(k,1);
58        f = MG.Converters(k,2);
59        if f==1 % fase a monofasico
60            DG(n,k) = 1;
61        end
62        if f==2 % fase b monofasico
63            DG(n+MG.NumN,k) = 1;
64        end
65        if f==3 % fase c monofasico
66            DG(n+2*MG.NumN,k) = 1;
67        end
68        if f==4 % las tres fases
69            DG(n,k) = 1/3;
70            DG(n+MG.NumN,k) = 1/3;
71            DG(n+2*MG.NumN,k) = 1/3;
72        end
73    end
74    Dg = DG(Ns,:);
75
76    % optimizacion
77    cvx_solver SeDuMi
78    cvx_precision high
79    cvx_begin quiet
80          variable Vn(MG.NumN*3-3,NumEsc) complex;
81          variable Si(MG.NumS,NumEsc) complex;
82          variable perdidas(NumEsc);
83          variable Valor_Esperado
84          variable xi(MG.NumS)
85    minimize Valor_Esperado;
```

```
86      subject to
87          Valor_Esperado == sum(Esc.Prob.*perdidas);
88          for k = 1:NumEsc
89              quad_form(Vn(:,k),YNN)+real(Vn(:,k)'*YN0*v0)+real(v0'*conj(YN0')*
                    Vn(:,k))+ real(v0'*Y00*v0) <= perdidas(k);
90             (Dg*Si(:,k)+Spn)== H*conj(Vn(:,k)) + M*Vn(:,k) + T;
91              abs(Si(:,k)) <= Smax*1.2;
92              real(Si(:,k))>= 0;
93              real(Si(:,k)) == Smax*Esc.Radiacion(k);
94              imag(Si(:,k)) == xi.*Smax*Esc.Radiacion(k);
95              abs(Vn(:,k)) <= 1.1;
96          end
97          xi <= 1;
98          xi >= -1;
99      cvx_end
100     rho = real(Si)./abs(Si);
101     rho(:,1)
102
103     for k = 1:NumEsc
104        Pslack(k) = real(v0'*(Y00*v0 + conj(YN0')*Vn(:,k)));
105     end
106
107     figure(3)
108     kk = 1:3*(MG.NumN-1);
109     plot(kk,abs(Vflujo),'--','LineWidth',2)
110     hold on
111     plot(kk,abs(Vn))
112     hold off
113     grid on
114     legend('No_PV','With_PV_Opt')
115     ylim([0.7 1.2])
116     xlim([0 55])
117     ylabel('Nodal_voltage_(pu)')
118     xlabel('Node')
119     grid on
120
121     Valor_Esperado
122     figure(4)
123     bar(perdidas)
124     hold on
125     plot(xlim,[Valor_Esperado Valor_Esperado],'r')
126     hold off
127     legend('Loss_by_Scenario','Expected_Value_of_Losses')
128     ylabel('P_{Loss}(pu)')
```

```
129     xlabel('Scenario')
130     grid on
131
132     figure(5)
133     bar(Pslack)
134     ylabel('P_{Slack}')
135     xlabel('Scenario')
136
137     figure(6)
138     p=plot(curva_demanda);
139     p(1).LineWidth = 2;
140     ylim([0  1.2])
141     xlim([0  25])
142     ylabel('Frequency')
143     xlabel('Time (h)')
144     grid on
145
146     time=toc
```

Bibliography

[Arif et al., 2017] Arif, M. A., Ndoye, M., Murphy, G. V., and Aganah, K. (2017). A stochastic game framework for reactive power reserve optimization and voltage profile improvement. In *2017 19th International Conference on Intelligent System Application to Power Systems (ISAP)*, pages 1–6.

[Arrillaga and Harker, 1983] Arrillaga, J. A. and Harker, B. J. (1983). *Computer Modelling of Electrical Power Systems*. John Wiley and Sons, Inc., New York, NY, USA, 1st edition.

[Bhattacharya et al., 2018] Bhattacharya, A., Kharoufeh, J. P., and Zeng, B. (2018). Managing energy storage in microgrids: A multistage stochastic programming approach. *IEEE Transactions on Smart Grid*, 9(1):483–496.

[Bolognani and Zampieri, 2013] Bolognani, S. and Zampieri, S. (2013). A distributed control strategy for reactive power compensation in smart microgrids. *IEEE Transactions on Automatic Control*, 58(11):2818–2833.

[Bolognani and Zampieri, 2016] Bolognani, S. and Zampieri, S. (2016). On the existence and linear approximation of the power flow solution in power distribution networks. *IEEE Transactions on Power Systems*, 31(1):163–172.

[Boyd and Vandenberghe, 2004] Boyd, S. and Vandenberghe, L. (2004). *Convex Optimization*. Cambridge University Press.

[Bullich-Massagué et al., 2018] Bullich-Massagué, E., Díaz-González, F., Aragüés-Peñalba, M., Girbau-Llistuella, F., Olivella-Rosell, P., and Sumper, A. (2018). Microgrid clustering architectures. *Applied Energy*, 212:340 – 361.

[Cai, 2018] Cai, G. (2018). Generation of correlated random variables and stochastic processes. *Probabilistic Engineering Mechanics*, 52:40 – 46.

[Casilimas et al., 2019] Casilimas, A., Montoya, O., and Garces, A. (2019). A convex formulation for optimal power factor correction in power electronic converters for photovoltaic applications. *Book*, 6.

[Conejo and Baringo, 2017] Conejo, A. and Baringo, L. (2017). Power system operations.

[D.A.Ramirez et al., 2019] D.A.Ramirez, A.Garces, and J.J.Mora (IEEE General Meeting 2019). A wirtinger linearization for the power flow in microgrids.

[Etherden and J.Bollen, 2011] Etherden, N. and J.Bollen, M. H. (2011). Increasing the hosting capacity of distribution networks by curtailment of renewable energy resources. In *2011 IEEE Trondheim PowerTech*, pages 1–7.

[Garces, 2016] Garces, A. (2016). A linear three-phase load flow for power distribution systems. *IEEE Transactions on Power Systems*, 31(1):827–828.

[Garces et al., 2012] Garces, A., Molinas, M., and Rodriguez, P. (2012). A generalized compensation theory for active filters based on mathematical optimization in abc frame. *Electric Power Systems Research*, 90:1 – 10.

[Gayatri et al., 2018] Gayatri, M., Parimi, A., and Kumar, A. P. (2018). A review of reactive power compensation techniques in microgrids. *Renewable and Sustainable Energy Reviews*, 81:1030 – 1036.

[Grant and Boyd, 2014] Grant, M. and Boyd, S. (2014). CVX: Matlab software for disciplined convex programming, version 2.1. `http://cvxr.com/cvx`.

[Grover-Silva et al., 2018] Grover-Silva, E., Heleno, M., Mashayekh, S., Cardoso, G., Girard, R., and Kariniotakis, G. (2018). A stochastic optimal power flow for scheduling flexible resources in microgrids operation. *Applied Energy*, 229:201 – 208.

[Guo et al., 2019] Guo, Y., Gao, H., Wu, Q., Østergaard, J., Yu, D., and Shahidehpour, M. (2019). Distributed coordinated active and reactive power control of wind farms based on model predictive control. *International Journal of Electrical Power and Energy Systems*, 104:78 – 88.

[Hamzeh et al., 2013] Hamzeh, M., Mokhtari, H., and Karimi, H. (2013). A decentralized self-adjusting control strategy for reactive power management in an islanded multi-bus mv microgrid. *Canadian Journal of Electrical and Computer Engineering*, 36(1):18–25.

[Han et al., 2017] Han, Y., Li, H., Shen, P., Coelho, E. A. A., and Guerrero, J. M. (2017). Review of active and reactive power sharing strategies in hierarchical controlled microgrids. *IEEE Transactions on Power Electronics*, 32(3):2427–2451.

[Hanhuawei et al., 2017] Hanhuawei, H., Chunli, W., Weiwei, J., Ning, S., Chuankun, L., Xinjiang, G., and Haozhi, W. (2017). A two-stage stochastic programming method for optimal power scheduling with solar power integration. In *2017 Chinese Automation Congress (CAC)*, pages 2041–2047.

[Kall and Wallace, 1994] Kall, P. and Wallace, S. (1994). *Stochastic Programming*, volume 46.

[Kekatos et al., 2015] Kekatos, V., Wang, G., Conejo, A. J., and Giannakis, G. B. (2015). Stochastic reactive power management in microgrids with renewables. *IEEE Transactions on Power Systems*, 30(6):3386–3395.

[Lin et al., 2012] Lin, M.-H., Tsai, J.-F., and Yu, C.-S. (2012). A review of deterministic optimization methods in engineering and management. *Mathematical Problems in Engineering*, 2012.

[Lu et al., 2015] Lu, W., Lang, S., Zhou, L., Iu, H. H., and Fernando, T. (2015). Improvement of stability and power factor in pcm controlled boost pfc converter with hybrid dynamic compensation. *IEEE Transactions on Circuits and Systems I: Regular Papers*, 62(1):320–328.

[Martí et al., 2013] Martí, J. R., Ahmadi, H., and Bashualdo, L. (2013). Linear power-flow formulation based on a voltage-dependent load model. *IEEE Transactions on Power Delivery*, 28(3):1682–1690.

[Morais et al., 2013] Morais, H., Sousa, T., Faria, P., and Vale, Z. (2013). Reactive power management strategies in future smart grids. In *2013 IEEE Power Energy Society General Meeting*, pages 1–5.

[(NREL), 2006] (NREL), T. N. R. E. L. (2006). Solar power data for integration studies. url: https://www.nrel.gov/grid/solar-power-data.html.

[Papathanassiou et al., 2005] Papathanassiou, S., Hatziargyriou, N., and Strunz, K. (2005). A benchmark low voltage microgrid network. *CIGRE Symposium*.

[Rabiul Islam et al., 2019] Rabiul Islam, M., Mahfuz-Ur-Rahman, A. M., Muttaqi, K. M., and Sutanto, D. (2019). State-of-the-art of the medium-voltage power converter technologies for grid integration of solar photovoltaic power plants. *IEEE Transactions on Energy Conversion*, 34(1):372–384.

[Razeghi et al., 2018] Razeghi, G., Gu, F., Neal, R., and Samuelsen, S. (2018). A generic microgrid controller: Concept, testing, and insights. *Applied Energy*, 229:660 – 671.

[Rylander et al., 2016] Rylander, M., Smith, J., and Sunderman, W. (2016). Streamlined method for determining distribution system hosting capacity. *IEEE Transactions on Industry Applications*, 52(1):105–111.

[Torquato et al., 2018] Torquato, R., Salles, D., Oriente Pereira, C., Meira, P. C. M., and Freitas, W. (2018). A comprehensive assessment of pv hosting capacity on low-voltage distribution systems. *IEEE Transactions on Power Delivery*, 33(2):1002–1012.

[Wang et al., 2016] Wang, S., Chen, S., Ge, L., and Wu, L. (2016). Distributed generation hosting capacity evaluation for distribution systems considering the robust optimal operation of oltc and svc. *IEEE Transactions on Sustainable Energy*, 7(3):1111–1123.

[Wang et al., 2017a] Wang, Y., Wang, X., Chen, Z., and Blaabjerg, F. (2017a). Distributed optimal control of reactive power and voltage in islanded microgrids. *IEEE Transactions on Industry Applications*, 53(1):340–349.

[Wang et al., 2017b] Wang, Y., Yu, Y., and Zhang, J. (2017b). Analysis for distribution network on hosting capacity of distributed wind turbines considering additional income under procedure conditions. *The Journal of Engineering*, 2017(13):1373–1377.

[Zhu et al., 2016] Zhu, Y., Zhuo, F., Wang, F., Liu, B., Gou, R., and Zhao, Y. (2016). A virtual impedance optimization method for reactive power sharing in networked microgrid. *IEEE Transactions on Power Electronics*, 31(4):2890–2904.

[Águila Téllez et al., 2018] Águila Téllez, A., López, G., Isaac, I., and González, J. (2018). Optimal reactive power compensation in electrical distribution systems with distributed resources. review. *Heliyon*, 4(8):e00746.